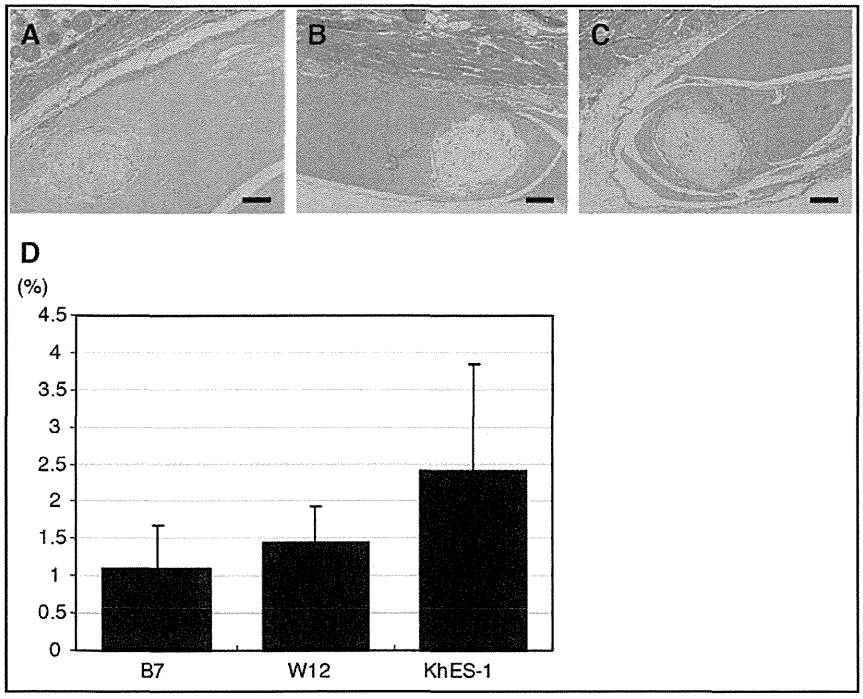


FIG. 6. Transplantation of adipocytes derived from other human pluripotent stem cells. **(A–C)** Transplanted cells were stained with HE. Morphological features of implanted Matrigel containing differentiated B7 **(A)**, W12 **(B)**, and KhES-1 **(C)** after 2 weeks. Scale bars = 100 μm. **(D)** Relative adipocyte areas at 2 weeks after transplantation of differentiated B7, W12, and KhES-1. Data are expressed as mean ± standard error. At least six sections from three samples were analyzed for each group.

mesenchymal progenitor cells are rare populations in differentiated iPS and ES cells after adipogenic induction at that point although mesenchymal progenitor cells may reside in derivatives from human PS cells at an earlier time point of this differentiation protocol.

Transplantation of mature adipocytes often results in graft loss caused by direct reduction of the number of viable adipocytes [22]. Transplantation of mature adipocytes together with adipose-derived stem cells significantly improves survival times and graft volumes, as compared with transplantation of mature adipocytes alone [21,44]. Thus, cotransplantation of mature adipocytes and preadipocytes derived from human iPS and ES cells may be advantageous for graft survival. Establishing a lineage-specific adipocyte differentiation protocol and the methods for the purification of adipocyte progenitors derived from human PS cells will be essential for the success of future cell therapies using adipocytes derived from human iPS cells.

Adipose tissue is now known to be a bona fide endocrine organ, which secretes a variety of adipocytokines, including leptin. Generalized lipodystrophy is caused by a profound deficiency in adipose tissue, which leads to diabetes with marked insulin resistance, hypertriglyceridemia, and ectopic lipid accumulation. We and others have established the efficacy and safety of long-term leptin replacement therapy for generalized lipodystrophy [45–50], but this therapy does not rescue these patients from their generalized lack of adipose tissue. The only complete cure for these patients would be replenishment of adipose tissue or adipocytes. Indeed, transplantation of adipose tissue or adipocyte progenitors has been demonstrated to ameliorate metabolic disorders in animal models of lipodystrophy [20,51]. Generalized lipodystrophy is classified into two types, congenital and acquired lipodystrophy. In the case of congenital lipodystrophy, we need to repair gene mutation of the patient-specific iPS cells for cell therapy. On the other hand, in the case of acquired lipodystrophy, iPS cells are expected to differentiate into adipocytes. However, successful engraftment of adipocytes derived from human iPS cells may be affected by host factors. Then, in consideration of allogeneic transplantation, iPS cell banking is now discussed, and some groups proposed clinical application of iPS cells from HLA homologous donors [52,53]. Transplantation using those allogeneic iPS cells can decrease or minimize the risk of immune rejection. Human iPS cell-derived adipocytes from patients or HLA homologous donors are a new strategy for the treatment of lipodystrophy.

In our transplantation studies, adipocytes derived from differentiated iPS (G4) and ES (H9) cells were clearly observed, whereas adipocytes derived from other human iPS cell lines (B7 and W12) or another human ES cell line (KhES-1) were observed less frequently. This suggests there is diversity among these cell lines with respect to the survival and maintenance of adipocytes. It was previously reported that there are marked differences in differentiation propensity among human ES cell lines [54]. One possible explanation is that these differences are attributable to the difference of in vitro adipogenic differentiation potential among these cell lines caused by their genetic backgrounds, sites of transgene integration, and epigenetic states. Further studies will be needed to clarify the mechanism underlying the observed differences.

In summary, the present study demonstrates that human iPS and ES cells can differentiate into adipocytes with functional properties and that adipocytes derived from human iPS and ES cells can survive and maintain the differentiated properties in vivo for at least 4 weeks after transplantation. Establishment of refined adipocyte differentiation protocol of human iPS and ES cells and the transplantation method of adipocytes derived from human iPS and ES cells will contribute to understanding the pathophysiology of metabolic

diseases such as obesity and lipodystrophy as well as to future therapeutic applications.

## Acknowledgments

We thank S. Yamanaka and K. Takahashi (Center for iPS Cell Research and Application) for providing human iPS cells and technical assistance of generating human iPS cells. We thank N. Nakatsuji (Institute for Frontier Medical Science, Kyoto University) for providing human ES cells. We thank A. Ryu and M. Nagamoto for technical assistance. This work was supported in part by research grants from the Ministry of Education, Culture, Sports, Science and Technology of Japan, including Grant-in-Aid for Scientific Research on Innovative Areas (research in a proposed research area). "Molecular Basis and Disorders of Control of Appetite and Fat Accumulation" research project no. 22126001; the Ministry of Health, Labour and Welfare of Japan; the Takeda Medical Research Foundation; the Smoking Research Foundation; Suzuken Memorial Foundation; Japan Foundation of Applied Enzymology; Novo Nordisk Insulin Research Award; and Lilly Education and Research Grant office.

## Author Disclosure Statement

The authors declare no potential conflict of interests.

## References

1. Takahashi K, K Tanabe, M Ohnuki, M Narita, T Ichisaka, K Tomoda and S Yamanaka. (2007). Induction of pluripotent stem cells from adult human fibroblasts by defined factors. Cell 131:861–872.
2. Yu J, MA Vodyanik, K Smuga-Otto, J Antosiewicz-Bourget, JL Frane, S Tian, J Nie, GA Jonsdottir, V Ruotti, et al. (2007). Induced pluripotent stem cell lines derived from human somatic cells. Science 318:1917–1920.
3. Park IH, R Zhao, JA West, A Yabuuchi, H Huo, TA Ince, PH Lerou, MW Lensch and GQ Daley. (2008). Reprogramming of human somatic cells to pluripotency with defined factors. Nature 451:141–146.
4. Chambers SM, CA Fasano, EP Papapetrou, M Tomishima, M Sadelain and L Studer. (2009). Highly efficient neural conversion of human ES and iPS cells by dual inhibition of SMAD signaling. Nat Biotechnol 27:275–280.
5. Dimos JT, KT Rodolfa, KK Niakan, LM Weisenthal, H Mitsumoto, W Chung, GF Croft, G Saphier, R Leibel, et al. (2008). Induced pluripotent stem cells generated from patients with ALS can be differentiated into motor neurons. Science 321:1218–1221.
6. Soldner F, D Hockemeyer, C Beard, Q Gao, GW Bell, EG Cook, G Hargus, A Blak, O Cooper, et al. (2009). Parkinson's disease patient-derived induced pluripotent stem cells free of viral reprogramming factors. Cell 136:964–977.
7. Osakada F, ZB Jin, Y Hirami, H Ikeda, T Danjyo, K Watanabe, Y Sasai and M Takahashi. (2009). *In vitro* differentiation of retinal cells from human pluripotent stem cells by small-molecule induction. J Cell Sci 122:3169–3179.
8. Choi KD, J Yu, K Smuga-Otto, G Salvagiotto, W Rehrauer, M Vodyanik, J Thomson and I Slukvin. (2009). Hematopoietic and endothelial differentiation of human induced pluripotent stem cells. Stem Cells 27:559–567.
9. Zhang J, GF Wilson, AG Soerens, CH Koonce, J Yu, SP Palecek, JA Thomson and TJ Kamp. (2009). Functional cardiomyocytes derived from human induced pluripotent stem cells. Circ Res 104:e30–e41.
10. Sullivan GJ, DC Hay, IH Park, J Fletcher, Z Hannoun, CM Payne, D Dalgetty, JR Black, JA Ross, et al. (2010). Generation of functional human hepatic endoderm from human induced pluripotent stem cells. Hepatology 51:329–335.
11. Hockemeyer D, F Soldner, EG Cook, Q Gao, M Mitalipova and R Jaenisch. (2008). A drug-inducible system for direct reprogramming of human somatic cells to pluripotency. Cell Stem Cell 3:346–353.
12. Maherali N, T Ahfeldt, A Rigamonti, J Utikal, C Cowan and K Hochedlinger. (2008). A high-efficiency system for the generation and study of human induced pluripotent stem cells. Cell Stem Cell 3:340–345.
13. Taura D, M Noguchi, M Sone, K Hosoda, E Mori, Y Okada, K Takahashi, K Homma, N Oyamada, et al. (2009). Adipogenic differentiation of human induced pluripotent stem cells: comparison with that of human embryonic stem cells. FEBS Lett 583:1029–1033.
14. Lian Q, Y Zhang, J Zhang, HK Zhang, X Wu, Y Zhang, FF Lam, S Kang, JC Xia, et al. (2010). Functional mesenchymal stem cells derived from human induced pluripotent stem cells attenuate limb ischemia in mice. Circulation 121:1113–1123.
15. Rhee YH, JY Ko, MY Chang, SH Yi, D Kim, CH Kim, JW Shim, AY Jo, BW Kim, et al. (2011). Protein-based human iPS cells efficiently generate functional dopamine neurons and can treat a rat model of Parkinson disease. J Clin Invest 121:2326–2335.
16. Liu H, Y Kim, S Sharkis, L Marchionni and YY Jang. (2011). *In vivo* liver regeneration potential of human induced pluripotent stem cells from diverse origins. Sci Transl Med 3:82ra39.
17. Nori S, Y Okada, A Yasuda, O Tsuji, Y Takahashi, Y Kobayashi, K Fujiyoshi, M Koike, Y Uchiyama, et al. (2011). Grafted human-induced pluripotent stem-cell-derived neurospheres promote motor functional recovery after spinal cord injury in mice. Proc Natl Acad Sci U S A 108:16825–16830.
18. Garg A. (2011). Clinical review#: Lipodystrophies: genetic and acquired body fat disorders. J Clin Endocrinol Metab 96:3313–3325.
19. Semple RK, DB Savage, EK Cochran, P Gorden and S O'Rahilly. (2011). Genetic syndromes of severe insulin resistance. Endocr Rev 32:498–514.
20. Gavrilova O, B Marcus-Samuels, D Graham, JK Kim, GI Shulman, AL Castle, C Vinson, M Eckhaus and ML Reitman. (2000). Surgical implantation of adipose tissue reverses diabetes in lipoatrophic mice. J Clin Invest 105:271–278.
21. ELFadl D, V Garimella, TK Mahapatra, PL McManus and PJ Drew. (2010). Lipomodelling of the breast: a review. Breast 19:202–209.
22. Chan CW, SJ McCulley and RD Macmillan. (2008). Autologous fat transfer—a review of the literature with a focus on breast cancer surgery. J Plast Reconstr Aesthet Surg 61:1438–1448.
23. Zeve D, W Tang and J Graff. (2009). Fighting fat with fat: the expanding field of adipose stem cells. Cell Stem Cell 5:472–481.
24. Locke M, V Feisst and PR Dunbar. (2011). Concise review: human adipose-derived stem cells: separating promise from clinical need. Stem Cells 29:404–411.
25. Alhadlaq A, M Tang and JJ Mao. (2005). Engineered adipose tissue from human mesenchymal stem cells maintains predefined shape and dimension: implications in soft tissue augmentation and reconstruction. Tissue Eng 11:556–566.
26. Choi YS, SN Park and H Suh. (2005). Adipose tissue engineering using mesenchymal stem cells attached to injectable PLGA spheres. Biomaterials 26:5855–5863.

27. Hong L, IA Peptan, A Colpan and JL Daw. (2006). Adipose tissue engineering by human adipose-derived stromal cells. Cells Tissues Organs 183:133–140.
28. Hillel AT, S Varghese, J Petsche, MJ Shamblott and JH Elisseeff. (2009). Embryonic germ cells are capable of adipogenic differentiation *in vitro* and *in vivo*. Tissue Eng Part A 15:479–486.
29. Thomson JA, J Itskovitz-Eldor, SS Shapiro, MA Waknitz, JJ Swiergiel, VS Marshall and JM Jones. (1998). Embryonic stem cell lines derived from human blastocysts. Science 282:1145–1147.
30. Suemori H, K Yasuchika, K Hasegawa, T Fujioka, N Tsuneyoshi and N Nakatsuji. (2006). Efficient establishment of human embryonic stem cell lines and long-term maintenance with stable karyotype by enzymatic bulk passage. Biochem Biophys Res Commun 345:926–932.
31. Noguchi M, K Hosoda, J Fujikura, M Fujimoto, H Iwakura, T Tomita, T Ishii, N Arai, M Hirata, et al. (2007). Genetic and pharmacological inhibition of Rho-associated kinase II enhances adipogenesis. J Biol Chem 282:29574–29583.
32. Tsuji W, T Inamoto, H Yamashiro, T Ueno, H Kato, Y Kimura, Y Tabata and M Toi. (2009). Adipogenesis induced by human adipose tissue-derived stem cells. Tissue Eng Part A 15:83–93.
33. Ahfeldt T, RT Schinzel, YK Lee, D Hendrickson, A Kaplan, DH Lum, R Camahort, F Xia, J Shay, et al. (2012). Programming human pluripotent stem cells into white and brown adipocytes. Nat Cell Biol 14:209–219.
34. Barberi T, LM Willis, ND Socci and L Studer. (2005). Derivation of multipotent mesenchymal precursors from human embryonic stem cells. PLoS Med 2:e161.
35. Xiong C, CQ Xie, L Zhang, J Zhang, K Xu, M Fu, WE Thompson, LJ Yang and YE Chen. (2005). Derivation of adipocytes from human embryonic stem cells. Stem Cells Dev 14:671–675.
36. Olivier EN, AC Rybicki and EE Bouhassira. (2006). Differentiation of human embryonic stem cells into bipotent mesenchymal stem cells. Stem Cells 24:1914–1922.
37. van Harmelen V, G Astrom, A Stromberg, E Sjolin, A Dicker, O Hovatta and M Ryden. (2007). Differential lipolytic regulation in human embryonic stem cell-derived adipocytes. Obesity (Silver Spring) 15:846–852.
38. Lian Q, E Lye, K Suan Yeo, E Khia Way Tan, M Salto-Tellez, TM Liu, N Palanisamy, RM El Oakley, EH Lee, B Lim and SK Lim. (2007). Derivation of clinically compliant MSCs from CD105+, CD24- differentiated human ESCs. Stem Cells 25:425–436.
39. Lee G, H Kim, Y Elkabetz, G Al Shamy, G Panagiotakos, T Barberi, V Tabar and L Studer. (2007). Isolation and directed differentiation of neural crest stem cells derived from human embryonic stem cells. Nat Biotechnol 25:1468–1475.
40. Mahmood A, L Harkness, HD Schroder, BM Abdallah and M Kassem. (2010). Enhanced differentiation of human embryonic stem cells to mesenchymal progenitors by inhibition of TGF-beta/activin/nodal signaling using SB-431542. J Bone Miner Res 25:1216–1233.
41. Ahmadian M, RE Duncan and HS Sul. (2009). The skinny on fat: lipolysis and fatty acid utilization in adipocytes. Trends Endocrinol Metab 20:424–428.
42. Gesta S, YH Tseng and CR Kahn. (2007). Developmental origin of fat: tracking obesity to its source. Cell 131:242–256.
43. Billon N, MC Monteiro and C Dani. (2008). Developmental origin of adipocytes: new insights into a pending question. Biol Cell 100:563–575.
44. Tremolada C, G Palmieri and C Ricordi. (2010). Adipocyte transplantation and stem cells: plastic surgery meets regenerative medicine. Cell Transplant 19:1217–1223.
45. Shimomura I, RE Hammer, S Ikemoto, MS Brown and JL Goldstein. (1999). Leptin reverses insulin resistance and diabetes mellitus in mice with congenital lipodystrophy. Nature 401:73–76.
46. Ebihara K, Y Ogawa, H Masuzaki, M Shintani, F Miyanaga, M Aizawa-Abe, T Hayashi, K Hosoda, G Inoue, et al. (2001). Transgenic overexpression of leptin rescues insulin resistance and diabetes in a mouse model of lipoatrophic diabetes. Diabetes 50:1440–1448.
47. Oral EA, V Simha, E Ruiz, A Andewelt, A Premkumar, P Snell, AJ Wagner, AM DePaoli, ML Reitman, et al. (2002). Leptin-replacement therapy for lipodystrophy. N Engl J Med 346:570–578.
48. Ebihara K, H Masuzaki and K Nakao. (2004). Long-term leptin-replacement therapy for lipoatrophic diabetes. N Engl J Med 351:615–616.
49. Ebihara K, T Kusakabe, M Hirata, H Masuzaki, F Miyanaga, N Kobayashi, T Tanaka, H Chusho, T Miyazawa, et al. (2007). Efficacy and safety of leptin-replacement therapy and possible mechanisms of leptin actions in patients with generalized lipodystrophy. J Clin Endocrinol Metab 92:532–541.
50. Nakao K, A Yasoda, K Ebihara, K Hosoda and M Mukoyama. (2009). Translational research of novel hormones: lessons from animal models and rare human diseases for common human diseases. J Mol Med 87:1029–1039.
51. Rodeheffer MS, K Birsoy and JM Friedman. (2008). Identification of white adipocyte progenitor cells *in vivo*. Cell 135:240–249.
52. Okita K, Y Matsumura, Y Sato, A Okada, A Morizane, S Okamoto, H Hong, M Nakagawa, K Tanabe, et al. (2011). A more efficient method to generate integration-free human iPS cells. Nat Methods 8:409–412.
53. Taylor CJ, S Peacock, AN Chaudhry, JA Bradley and EM Bolton. (2012). Generating an iPSC bank for HLA-matched tissue transplantation based on known donor and recipient HLA types. Cell Stem Cell 11:147–152.
54. Osafune K, L Caron, M Borowiak, RJ Martinez, CS Fitz-Gerald, Y Sato, CA Cowan, KR Chien and DA Melton. (2008). Marked differences in differentiation propensity among human embryonic stem cell lines. Nat Biotechnol 26:313–315.

Address correspondence to:
*Dr. Kiminori Hosoda*
*Department of Medicine and Clinical Science*
*Kyoto University Graduate School of Medicine*
*54 Shogoin Kawahara-cho, Sakyo-ku*
*Kyoto 606-8507*
*Japan*

*E-mail:* kh@kuhp.kyoto-u.ac.jp

*Dr. Kazuwa Nakao*
*Department of Medicine and Clinical Science*
*Kyoto University Graduate School of Medicine*
*54 Shogoin Kawahara-cho, Sakyo-ku*
*Kyoto 606-8507*
*Japan*

*E-mail:* nakao@kuhp.kyoto-u.ac.jp

Received for publication February 27, 2013
Accepted after revision June 10, 2013
Prepublished on Liebert Instant Online June 10, 2013

**Original Article**
CLINICAL TRIALS: BEHAVIOR, PHARMACOTHERAPY, DEVICES, SURGERY

Obesity

# Early Changes of Abdominal Adiposity Detected with Weekly Dual Bioelectrical Impedance Analysis during Calorie Restriction

*Midori Ida[1], Masakazu Hirata[1], Shinji Odori[1], Eisaku Mori[1], Eri Kondo[1], Junji Fujikura[1], Toru Kusakabe[1], Ken Ebihara[1], Kiminori Hosoda[1,2] and Kazuwa Nakao[1]*

**Objective:** To elucidate early change of intra-abdominal fat in response to calorie restriction in patients with obesity by weekly evaluation using a dual bioelectrical impedance analysis (Dual BIA) instrument.
**Design and Methods:** For 67 Japanese patients with obesity, diabetes, or metabolic syndrome, intra-abdominal fat area (IAFA), initially with both Dual BIA and computed tomography (CT), and in subsequent weeks of calorie restriction, with Dual BIA were measured.
**Results:** IAFA by Dual BIA (Dual BIA-IAFA) correlated well with IAFA by CT (CT-IAFA) in obese patients ($r = 0.821$, $P < .0001$, $n = 67$). Ten males and 9 females (age 49.0 ± 14.4 years, BMI 33.2 ± 7.3 kg/m$^2$) lost more than 5% of baseline body weight (BW) in 3 weeks, and their Dual BIA-IAFA, BW, and WC decreased by 18.9%, 5.3%, and 3.8%, respectively ($P < .05$, ANCOVA).
**Conclusion:** Dual BIA instrument could detect the weekly change of Dual BIA-IAFA under calorie restriction in obese patients and demonstrated a substantially larger change of IAFA compared with changes of BW and WC in early weeks. This observation corroborates the significance of evaluating IAFA as a biomarker for obesity, and indicates the clinical usefulness of the Dual BIA instrument.

*Obesity* (2013) **21**, E350-E353. doi:10.1002/oby.20300

## Introduction

Abdominal adiposity is associated with development of obesity and metabolic abnormalities in obesity-related diseases (1-3). The adipose tissue distribution has been quantitatively evaluated by computed tomography (CT) (4) or magnetic resonance imaging (MRI) (5), and intra-abdominal fat area (IAFA) is used as a clinical parameter of abdominal adiposity (6). Although waist circumference (WC) is casually employed to evaluate abdominal adiposity (7), WC is known to reflect both the intra-abdominal and the subcutaneous abdominal adiposity. In addition, the correlation of WC with intra-abdominal adiposity is influenced by age and sex as shown in epidemiological studies (5). Thus, WC does not necessarily provide the precise information about abdominal fat distribution. Therefore, a new practical method for detecting early change in abdominal adiposity is needed to elucidate its consequence during acute phase of calorie restriction in obesity treatment (8). There have been a few proposals of methods (9,10) that assess IAFA as alternatives to CT (4) or MRI (5). However, there has been no report on clinical application of these methods analyzing the weekly change of IAFA during calorie restriction. We have developed the dual bioelectrical impedance analysis (Dual BIA) instrument that can determine IAFA by measuring truncal impedance and surface impedance at the abdomen separately, each of which reflects the truncal adiposity and the subcutaneous adiposity respectively (11-13). The Dual BIA instrument has been optimized with aims at robustness for use in a wide range of human variation by analyzing the size of effect that each parameter, such as age and gender, can have on the calculation outcomes utilizing information technology (11-13). In this study, we report on application of the Dual BIA instrument to compare the weekly change in IAFA and body weight (BW) of obese patients with the metabolic syndrome or diabetes mellitus resulting from calorie restriction.

## Methods

### Dual BIA method and instrumentation

Dual BIA instrument calculates the cross-sectional area of intra-abdominal fat at the level of umbilicus based on the measurement of electrical potentials resulting from applying small electrical currents in two different body space. Principles of IAFA determination by Dual BIA instrument have been described previously (11-13) in detail. Briefly, the Dual BIA instrument consists of bioelectrical impedance

[1] Department of Medicine and Clinical Science, Kyoto University Graduate School of Medicine, Sakyo-ku, Kyoto, Japan. Correspondence: Masakazu Hirata (mhirata@kuhp.kyoto-u.ac.jp) [2] Department of Human Health Science, Kyoto University Graduate School of Medicine, Sakyo-ku, Kyoto, 606-8507, Japan

**Disclosure:** The authors declared no conflict of interest.
**Funding agencies:** This work was supported in part by research grants from the Ministry of Education, Culture, Sports, Science and Technology of Japan including Grant in Aid for Scientific Research on Innovative Areas (Research in a proposed research area) "Molecular Basis and Disorders of Control of Appetite and Fat Accumulation", the Ministry of Health, Labour and Welfare of Japan, the Takeda Medical Research Foundation, the Smoking Research Foundation, Suzuken Memorial Foundation, Japan Foundation of Applied Enzymology, Novo Nordisk Insulin Research Award, Lilly Education and Research Grant Office.
**Received:** 8 May 2012 **Accepted:** 25 November 2012 **Published online 2 January 2013. doi:10.1002/oby.20300**

component that measures truncal and surface impedance of the body, and a device that measures physical size of the abdomen. The two sets of electrodes are for limb and truncal placement. The limb electrodes consist of four clip-on electrodes placed on wrists and ankles. The truncal electrodes are eight pairs of electrodes 6 cm apart longitudinally that are fixed to a belt where four pairs each for front and back are positioned at an equal inter-electrode distance. The belt is adjustable so that the electrodes are positioned centered on mid-sagittal line at the level of umbilicus in supine position. The truncal impedance is measured by applying electrical currents between upper and lower limb leads and reading voltage from the electrodes around the abdominal circumference. The surface impedance is measured by applying and reading voltage from the abdominal circumferential electrodes. IAFA by Dual BIA (Dual BIA-IAFA) is calculated as follows.

$$\text{Dual BIA} - \text{IAFA} = \alpha_1 A + \alpha_2 B^2 - \alpha_3 \left(A^2 + B^2\right)^{1/2} Z_s - \alpha_4 / Z_t + \varepsilon \quad (1)$$

$A$: abdominal antero-posterior diameter, $B$: abdominal transverse diameter, $Z_s$: surface impedance, $Z_t$: truncal impedance, $\varepsilon$: residual constant.

There was a good agreement of Dual BIA-IAFA and IAFA measured by CT (CT-IAFA) with the correlation coefficient of 0.888 ($n = 98$, $P < .001$) (13).

## Patient selection

The study was performed according to the protocol approved by Kyoto University Medical Ethics Review Board (no. 080116). The patient gave a written consent to participate in this study which took place at the endocrinology and metabolism ward of Kyoto University Hospital. We collected data from 67 Japanese patients (36 males and 31 females; mean ± SD age, 54.7 ± 14.7 years, BMI 29.3 ± 6.5 kg/m$^2$) with obesity ($n = 56$), diabetes mellitus ($n = 45$), or the metabolic syndrome ($n = 38$) who were hospitalized for calorie restriction therapy or diet education, and had measurement of IAFA by both Dual BIA method and CT method at the start of calorie restriction. Obesity was diagnosed as BMI 25.0, and metabolic syndrome was diagnosed according to 2005 Japanese criteria of metabolic syndrome (14). Average daily calorie intake was 1437.3 ± 201.4 kcal/day (19.3 ± 4.3 kcal/ideal BW). Out of 67 patients, 35 patients could be followed for longer than 3 weeks, while the other patients were discharged earlier after examination of complications and diet and lifestyle education. Total daily energy was varied individually during hospitalization based on consultation between the patient, a dietician, and a physician. Out of 35 patients who had their Dual BIA-IAFA monitored every week for at least 3 weeks (four times), 19 patients lost more than 5% of baseline BW, and were included in the analysis of weekly change in Dual BIA-IAFA, WC, and BW during weight reduction.

## Measurement of Dual BIA, CT, and anthropometric parameters

Dual BIA-IAFA was measured every week in the morning before breakfast depending on individual patient's treatment schedule (Figure 1A). Abdominal CT was performed for calculation of CT-IAFA within 7 days before the initial Dual BIA-IAFA measurement. CT-IAFA was calculated at umbilical level by the software, Virtual Place Lexus (AZE of Japan, Ltd). BW was measured to the nearest 0.1 kg in the morning of the Dual BIA-IAFA measurement.

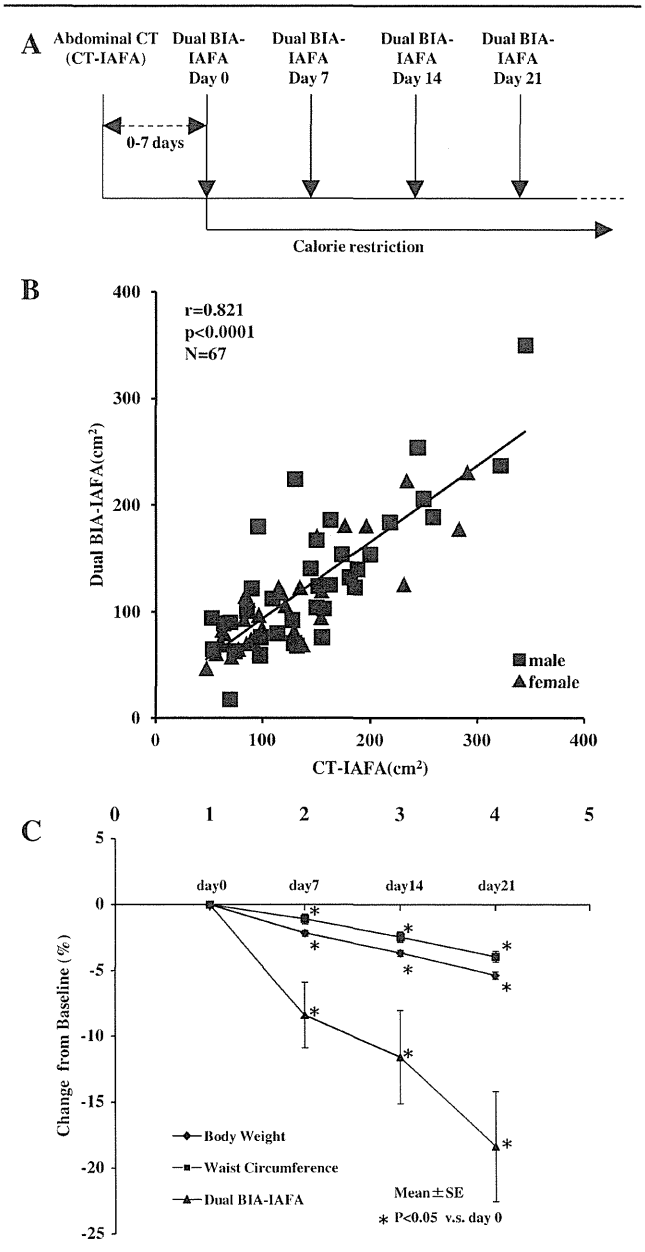


**FIGURE 1 A**: Diagram of IAFA assessment schedule during the calorie restriction. Patients started fixed calorie diet within 7 days of taking the abdominal CT image. Dual BIA-IAFA assessment took place in the morning before meal every week. CT imaging took place either in the morning or in the afternoon. **B**: Correlation between CT-IAFA and BIA-IAFA in 67 patients who were with obesity-related disorders. Square symbols: male, Triangle symbols: female. $r = 0.821$, $P < .001$ by Pearson's analysis. **C**: Weekly change of Dual BIA-IAFA plotted along with BW and WC during weight loss. Nineteen patients who underwent the calorie restriction and had abdominal CT examined at baseline were monitored for their anthropometric parameters and Dual BIA-IAFA weekly for at least 3 weeks. They lost more than 5% of BW during the period. Size of the change from baseline values (mean ± SE) is expressed as %. *$P < .05$ by Student's paired $t$-test.

WC was measured at the level of the umbilicus to the nearest 0.1 cm in the standing position at the end of expiration while breathing gently at the time of Dual BIA measurement.

### Statistical methods

Correlation between values obtained by Dual BIA and CT were evaluated using Pearson's correlation analysis. Weekly values of Dual BIA-IAFA, BW, and WC were compared with the baseline values of day 0 by Student's paired *t*-test. Analysis of covariance was applied for comparison of Dual BIA-IAFA, BW, and WC at week 3.

## Results

In 67 patients with obesity and related conditions, Dual BIA-IAFA correlated well with CT-IAFA ($r = 0.821$, $P < .0001$) (Figure 1B).

Thirty-five (17 males and 18 females) out of 67 patients were monitored with Dual BIA for longer than 3 weeks, and 19 (10 males and 9 females) out of 35 patients achieved weight loss of more than 5% of the initial BW. In order to elucidate the change in IAFA during weight loss, Dual BIA-IAFA, BW, and WC of the 19 patients were analyzed. Baseline characteristics of the 19 patients were (mean ± SD); age, 49.0 ± 14.4 years, height 163.0 ± 10.5 cm, BMI 33.2 ± 7.3 kg/m$^2$, and CT-IAFA 143.6 ± 47.4 cm$^2$. BW, WC, and Dual BIA-IAFA at baseline and at week 3 were: 89.2 ± 26.2 kg and 84.5 ± 25.1 kg, 110.6 ± 14.1 cm and 106.0 ± 14.2 cm, and 150.4 ± 73.7 cm$^2$ and 124.3 ± 70.3 cm$^2$, respectively.

Figure 1C shows the weekly change of Dual BIA-IAFA, BW, and WC in 19 patients whose BW decreased more than 5% during the 3 weeks of monitoring. Dual BIA-IAFA, BW and WC showed a significant reduction after 1 week during the calorie restriction compared with the baseline values ($P < .05$). Dual BIA-IAFA decreased every week for the initial 3 weeks and the average reduction in Dual BIA-IAFA was 18.9%, which was larger than in BW (5.3%) and WC (3.8%) (ANCOVA, $P < .05$).

## Discussion

The present study demonstrates that the weekly change in IAFA can be detected with the Dual BIA instrument during the calorie restriction. Due to the practical limitations such as instrumentation and cost, CT and MRI are unsuitable for weekly monitoring of change in IAFA. There is also a problem of X-ray exposure in CT scanning. Consequently, it has been impractical to monitor IAFA weekly or frequently, in clinical follow-up period with CT or MRI. There have been several attempts to evaluate the IAFA by BIA (9-13). They include calculation from whole body impedance and from measuring abdominal impedance by the electrodes placed on the abdomen (9,10). Some of the estimates of IAFA incorporate gender and age of the subject in order to attain high correlation with CT (9,10). In contrast, Dual BIA, which is a method that is not dependent on external variables, such as gender or age, had shown a good correlation between Dual BIA-IAFA and CT-IAFA (11-13). In the present study, we confirmed the good correlation of Dual BIA-IAFA and CT-IAFA in obese patients. The correlation coefficient for the Dual BIA-IAFA and CT-IAFA was 0.821 ($n = 67$) with our subjects whose average BMI was 29.3. This indicates that Dual BIA produced reliable measurements with obesity patients and the result was comparable to the correlation coefficient of 0.888 obtained with subjects whose average BMI was around 25 (13). It must be noted that CT-IAFA and Dual BIA-IAFA was not measured on the same day in the present study, unlike the previous report in which Dual BIA- and CT-IAFA was taken on the same day (13), and therefore direct comparison has its limitations. By applying Dual BIA to monitoring the weekly change of individual body component during the calorie restriction, we could detect the characteristic change of IAFA. The significant decrease in Dual BIA-IAFA, BW, and WC at week 1 supports the suitability of selecting 5% of BW change at week 3 as a criterion for including in weekly analysis of these parameters.

On average, IAFA showed a larger reduction than BW and WC during the initial 3 weeks of calorie restriction. The rapid response of intra-abdominal adipose tissue to calorie restriction has been suggested in an ultrasonography study that examined a portion of peritoneal fat thickness (15). The larger decrease of Dual BIA-IAFA observed is also in agreement with a study which showed larger reduction in IAFA evaluated with MRI than that of BW up to 12 weeks on very low calorie diet (16). Together with these results, the present study established that the intra-abdominal fat decreases rapidly in the initial period of calorie restriction by measuring Dual BIA-IAFA, and demonstrates the usefulness of monitoring the change in IAFA during the treatment of obesity and its related disorders.

Weakness of our study is that its design was not of a prospective weight reduction where every participant was prescribed daily calorie that could produce predetermined level of weight loss within the study period. Instead we selected participants that had their weight decreased by at least 5% in order to illustrate the change in abdominal adiposity on weekly basis. It is also of note that the BW and Dual BIA-IAFA at week 1 may be affected by salt restriction and loss of body water that is observed early in calorie restriction. Because of the small sample size, the observed change in Dual BIA-IAFA could be larger than actual change. It also depends on the precision of the instrument. In a separate population, the coefficient of variation was 7.6% (Ida, M. manuscript in preparation).

In conclusion, the present study demonstrated that Dual BIA instrument can be used to measure IAFA in obese patients, allows frequent measurement, and is useful for detecting the early change in IAFA during calorie restriction. Information thus obtained along with other changes in metabolic parameters will be indispensable for understanding the role of abdominal adiposity, and especially useful as a diagnostic marker for monitoring obesity and its related disorders (1). In addition, the instrument's safety and convenience could be suitable for large population studies.O

## Acknowledgments

Authors thank all the volunteers who took part in the study, and Research and Development Department of Omron Healthcare Corporation for use of the Dual BIA instrument.



## References

1. Matsuzawa Y. The role of fat topology in the risk of disease. *Int J Obes* 2008;32: S83-S92.

2. Miyawaki T, Hirata M, Moriyama K, et al. Metabolic syndrome in Japanese diagnosed with visceral fat measurement by computed tomography. *Proc Jpn Acad Ser B* 2005;81:471-479.
3. Després JP, Lemieux I. Abdominal obesity and metabolic syndrome. *Nature* 2006; 444:881-887.
4. Ferland M, Després JP, Trembly A, et al. Assessment of adipose tissue distribution by computed axial tomography in obese women: association with body density and anthropometric measurements. *Br J Nutr* 1989;61:139-148.
5. Kuk JL, Lee S, Heymsfield SB, Ross R. Waist circumference and abdominal adipose tissue distribution: influence of age and sex. *Am J Clin Nutr* 2005;81: 1330-1334.
6. Cornier MA, Després JP, Davis N, et al. A scientific statement from the American Heart Association. *Circulation* 2011;124:1996-2019.
7. Miyawaki T, Abe M, Yahata K, Kajiyama N, Katsuma H, Saito N. Contribution of visceral fat accumulation to the risk factors for atherosclerosis in non-obese Japanese. *Intern Med* 2004;43:1138-1144.
8. Isbess JM, Tamboli RA, Hansen EN, et al. The importance of caloric restriction in the early improvements in insulin sensitivity after Roux-en Y gastric bypass surgery. *Diabetes Care* 2010;33:1438-1442.
9. Ryo M, Maeda K, Onda T, et al. A new simple method for the measurement of visceral fat accumulation by bioelectrical impedance. *Diabetes Care* 2005;8:451-453.
10. Nagai M, Komiya H, Mori Y, Ohta T, Kasahara Y, Ikeda Y. Development of a new method for estimating visceral fat area with multi-frequency bioelectrical impedance. *Tohoku J Exp Med* 2008;214:105-112.
11. Shiga T, Oshima Y, Kanai H, Hirata M, Hosoda K, Nakao K. *A simple measurement method of visceral fat accumulation by bioelectrical impedance analysis*, In: *IFMBE Proceedings*, Vol. 17/14: 13th International Conference on Electrical Bioimpedance and the 8th Conference on Electrical Impedance Tomography; Scharfetter H, et al., eds., Springer-Verlag; 2007, pp 687-690.Available at: http://link.springer.com/chapter/10.1007%2F978-3-540-73841-1_177?LI=true.
12. Yoneda M, Tasaki H, Tsuchiya N, et al. A study of bioelectrical impedance analysis methods for practical visceral fat estimation. In: IEEE International Conference on Granular Computing (GCR 2007), Lin TY, et al., eds., IEEE Computer Society Press; 2007, pp 622-627. Available at: http://ieeexplore.ieee.org/xpl/login.jsp?tp=&arnumber=4403174&url=http%3A%2F%2Fieeexplore.ieee.org%2Fxpls%2Fabs_all.jsp%3Farnumber%3D4403174.
13. Shiga T, Hamaguchi T, Oshima Y, et al. *A new simple measurement system of visceral fat accumulation by bioelectrical impedance analysis*. In *IFMBE Proceedings* Vol. 25/7: World Congress on Medical Physics and Biomedical Engineering, Döossel O, et al., eds., Springer-Verlag; 2009, pp 338-341.
14. Matsuzawa Y. Metabolic syndrome—definition and diagnostic criteria in Japan. *J Atheroscler Thromb* 2005;12:301.
15. Li Y, Bujo H, Takahashi K, et al. Visceral Fat: higher responsiveness of fat mass and gene expression to calorie restriction than subcutaneous fat. *Exp Biol Med (Maywood)* 2003;228:1118-1123.
16. Colles SL, Dixon JB, Marks P, et al. Preoperative weight loss with a very-low-energy diet: quantitation of changes in liver and abdominal fat by serial imaging. *Am J Clin Nutr* 2006;84:304-311.

# Intracerebroventricular Administration of C-Type Natriuretic Peptide Suppresses Food Intake via Activation of the Melanocortin System in Mice

Nobuko Yamada-Goto,[1] Goro Katsuura,[1] Ken Ebihara,[1] Megumi Inuzuka,[1] Yukari Ochi,[1] Yui Yamashita,[1] Toru Kusakabe,[1] Akihiro Yasoda,[1] Noriko Satoh-Asahara,[2] Hiroyuki Ariyasu,[1] Kiminori Hosoda,[1] and Kazuwa Nakao[1]

C-type natriuretic peptide (CNP) and its receptor are abundantly distributed in the brain, especially in the arcuate nucleus (ARC) of the hypothalamus associated with regulating energy homeostasis. To elucidate the possible involvement of CNP in energy regulation, we examined the effects of intracerebroventricular administration of CNP on food intake in mice. The intracerebroventricular administration of CNP-22 and CNP-53 significantly suppressed food intake on 4-h refeeding after 48-h fasting. Next, intracerebroventricular administration of CNP-22 and CNP-53 significantly decreased nocturnal food intake. The increment of food intake induced by neuropeptide Y and ghrelin was markedly suppressed by intracerebroventricular administration of CNP-22 and CNP-53. When SHU9119, an antagonist for melanocortin-3 and melanocortin-4 receptors, was coadministered with CNP-53, the suppressive effect of CNP-53 on refeeding after 48-h fasting was significantly attenuated by SHU9119. Immunohistochemical analysis revealed that intracerebroventricular administration of CNP-53 markedly increased the number of c-Fos–positive cells in the ARC, paraventricular nucleus, dorsomedial hypothalamus, ventromedial hypothalamic nucleus, and lateral hypothalamus. In particular, c-Fos–positive cells in the ARC after intracerebroventricular administration of CNP-53 were coexpressed with α-melanocyte–stimulating hormone immunoreactivity. These results indicated that intracerebroventricular administration of CNP induces an anorexigenic action, in part, via activation of the melanocortin system. ***Diabetes* 62:1500–1504, 2013**

C-type natriuretic peptide (CNP) is a member of the natriuretic peptide family and has been demonstrated to be abundantly present in the brain, interestingly in discrete hypothalamic areas, such as the arcuate nucleus (ARC) of the hypothalamus, that play pivotal roles in energy regulation (1–3). Two predominant molecular forms of CNP in the porcine brain were reported to be a 22-residue peptide (CNP-22) and its *N*-terminally elongated 53-residue peptide (CNP-53) (1). Moreover, natriuretic peptide receptor-B (NPR-B), a CNP receptor, is also widely distributed in the brain and is reported to be abundantly expressed in the ARC of the hypothalamus (4,5). These findings indicate the possibility that the brain CNP/NPR-B system may regulate energy homeostasis.

In the current study, we examined the effects of intracerebroventricular administration of CNP on food intake induced by refeeding after fasting and by orexigenic peptides, such as neuropeptide Y (NPY) and ghrelin. Also, we examined the involvement of the melanocortin system in the CNP actions.

## RESEARCH DESIGN AND METHODS

**Animals and diets.** Male C57BL/6J mice (6 weeks old) obtained from Japan SLC (Shizuoka, Japan) were housed in plastic cages in a room kept at a room temperature of 23 ± 1°C and a 12:12-h light–dark cycle (lights turned on at 9:00 A.M.). The mice had ad libitum access to water and food (CE-2; CLEA Japan, Tokyo, Japan). All experiments were performed at 10 weeks of age in accordance with the guidelines established by the Institutional Animal Investigation Committee at Kyoto University and the United States National Institutes of Health Guide for the Care and Use of Laboratory Animals. Every effort was made to optimize comfort and to minimize the use of animals.

**Peptides.** CNP-22, CNP-53, ghrelin, and NPY were purchased from Peptide Institute (Osaka, Japan). SHU9119 was purchased from Bachem AG (Bubendorf, Switzerland).

**Intracerebroventricular injection.** Intracerebroventricular injection was performed according to our previous report (6).

**Measurement of food intake**

***Fasting-refeeding.*** Mice were fasted for 48 h and then refed for 4 h. Water was available ad libitum during the experiments. The intracerebroventricular or intraperitoneal administration of CNP-22 or CNP-53 was performed just before refeeding. Food intake was measured for 4 h of refeeding. At the end of experiments, the hypothalamus was collected for examination of the expressions of mRNA for neuropeptides (7).

***Nocturnal food intake.*** To assess the effect of intracerebroventricular administration of CNP-22 or CNP-53 on nocturnal food intake, peptides were injected intracerebroventricularly 1 h before the beginning of the dark phase. Food intake was measured for 15 h after intracerebroventricular injection. Water was available ad libitum during the experiments.

***Food intake induced by NPY and ghrelin.*** The experiments were performed from 11:00 A.M. to 3:00 P.M. CNP-22 or CNP-53 was intracerebroventricularly administrated just before intracerebroventricular injection of NPY (5 nmol/mouse) or intraperitoneal injection of ghrelin (100 nmol/kg). Food intake was measured for 4 h after peptide injection. In these experiments, food and water were available ad libitum.

**PCR.** The extraction of mRNA and quantitative real-time RT-PCR were performed according to our previous report (8). Primers for preopiomelanocortin, cocaine and amphetamine-related peptide, *NPY*, agouti gene-related peptide (*AgRP*) and glyceraldehyde 3-phosphate dehydrogenase are shown in Supplementary Table 1.

**Immunohistochemistry for c-Fos and α-MSH in the hypothalamus.** The immunohistochemical methods and the stereotaxic coordinates for the hypothalamic nuclei were based on our previous report (6). Briefly, mice were anesthetized with pentobarbital at 1 h after intracerebroventricular injection of CNP-53 (1.5 nmol/mouse) and perfused with 50 mL 0.1 mol/L PBS, followed by 50 mL ice-cold 4% paraformaldehyde in 0.1 mol/L PBS. Sections of 30-μm thickness were cut with a cryostat. According to the mouse brain atlas (9), cross-sections were selected in correspondence to −1.70 mm [ARC, lateral hypothalamus (LH), dorsomedial hypothalamus (DMH), ventromedial hypothalamic

From the [1]Department of Medicine and Clinical Science, Kyoto University Graduate School of Medicine, Kyoto, Japan; and the [2]Clinical Research Institute, National Hospital Organization, Kyoto Medical Center, Kyoto, Japan.
Corresponding author: Nobuko Yamada-Goto, nobukito@kuhp.kyoto-u.ac.jp.
Received 31 May 2012 and accepted 7 November 2012.
DOI: 10.2337/db12-0718
This article contains Supplementary Data online at http://diabetes.diabetesjournals.org/lookup/suppl/doi:10.2337/db12-0718/-/DC1.


**See accompanying commentary, p. 1379.**

nucleus (VMH)] and to −0.82 mm [paraventricular nucleus (PVN)], relative to bregma. For c-Fos and α-melanocyte–stimulating hormone (α-MSH) protein staining, the sections were incubated with antic-Fos rabbit antibody (Ab-5; 1:5,000; Oncogene Science, Cambridge, MA) and antiα-MSH sheep antibody (AB5087; 1:10,000; EMD Millipore, Billerica, MA), respectively. The antibody was detected using the Vectastain ABC Elite kit (PK-6101; Vector Laboratories, Burlingame, CA) and a diaminobenzidine substrate kit (SK-4100; Vector Laboratories) was used for visualization. The second antibodies for fluorescence visualization used were goat anti-rabbit488 (A11008; 1:200; Life Technologies, Carlsbad, CA) for antic-Fos rabbit antibody and goat anti-sheep546 (A21098; 1:200; Life Technologies) for antiα-MSH sheep antibody.

**Data analysis.** All values are given as the mean ± SEM. Statistical analysis of the data were performed by ANOVA, followed by the Tukey-Kramer test. Statistical significance was defined as $P < 0.05$.

## RESULTS

**Effects of intracerebroventricular administration of CNP-22 and CNP-53 on food intake at refeeding after fasting.** The intracerebroventricular administration of CNP-22 (1.5 and 4.5 nmol/mouse) and CNP-53 (1.5 nmol/mouse) significantly suppressed food intake during 4-h refeeding after 48-h fasting in comparison with data from saline-treated mice (Fig. 1*A*). In this experiment, CNP-53 (1.5 nmol), but not other treatments, induced significant reduction of body weight compared with saline treatment (Supplementary Table 2). The mRNA expressions of preopiomelanocortin and cocaine and amphetamine-related peptide significantly decreased, and the mRNA expressions of *NPY* and *AgRP* significantly increased after refeeding compared with control animals (Supplementary Fig. 1). The intracerebroventricular administration of CNP-53 did not influence the mRNA expressions of these neuropeptides in the hypothalamus (Supplementary Fig. 1). Next, the peripheral action of CNP on food intake was examined when a 10-fold greater dose than intracerebroventricular injection of each CNP was intraperitoneally administered. The intraperitoneal administrations of CNP-22 (1.5 μmol/kg) and CNP-53 (0.5 μmol/kg) did not change the food intake during 4-h refeeding after 48-h fasting (Fig. 1*B*), nor were there changes in body weight (Supplementary Table 3).

The intracerebroventricular administrations of CNP-22 (4.5 nmol/mouse) and CNP-53 (1.5 nmol/mouse) at 1 h before the start of the dark phase significantly suppressed nocturnal food intake compared with saline treatment (Fig. 1*C*).

**Effect of intracerebroventricular administration of CNP-22 and CNP-53 on NPY-induced and ghrelin-induced food intake.** When CNP-22 (4.5 nmol/mouse) and CNP-53 (1.5 nmol/mouse) were concomitantly administered intracerebroventricularly with NPY, they significantly suppressed the food intake induced by NPY compared with that of saline treatment (Fig. 2*A*). When CNP-22 (4.5 nmol/mouse) and CNP-53 (1.5 nmol/mouse) were administered intracerebroventricularly with ghrelin, they significantly suppressed the food intake induced by ghrelin compared with that of saline treatment (Fig. 2*B*).

**Effect of melanocortin receptor antagonist, SHU9119, on the anorectic effect of CNP.** To examine its involvement in the anorectic effect of CNP, SHU9119 was administered intracerebroventricularly together with CNP-53 (1.5 nmol/mouse). SHU9119 (1 nmol/mouse) significantly attenuated the suppressive action of CNP-53 on the food intake during 4-h refeeding after 48-h fasting, whereas SHU9119 itself significantly enhanced the increase of food intake in comparison with mice administered saline treatment (Fig. 3).

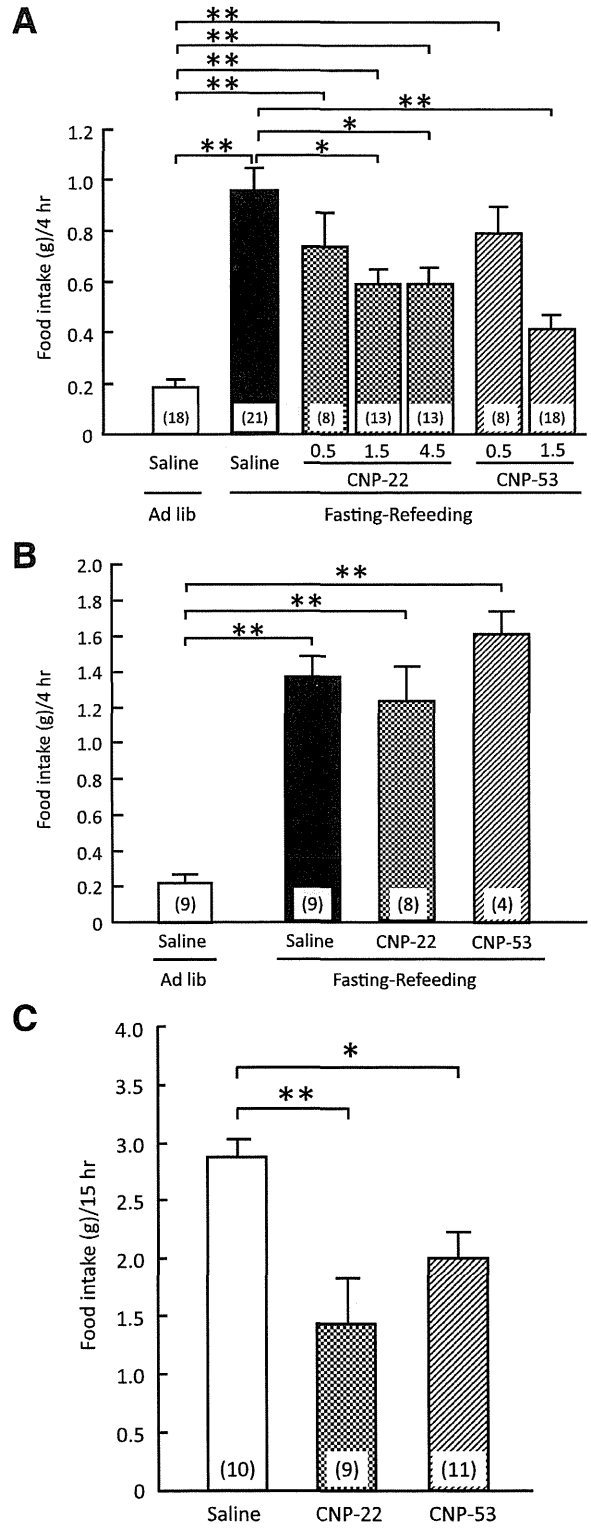


**FIG. 1. Effects of CNP on refeeding after fasting. *A*: Effects of intracerebroventricular administration of CNP-22 (0.5, 1.5, and 4.5 nmol/mouse) and CNP-53 (0.5 and 1.5 nmol/mouse) on 4-h refeeding after 48-h fasting in mice. Food intake was observed for 4 h after refeeding. *B*: Effects of intraperitoneal administration of CNP-22 (1.5 μmol/kg) and CNP-53 (0.5 μmol/kg) on 4-h refeeding after 48-h fasting in mice. Food intake was observed for 4 h after refeeding. *C*: Effects of intracerebroventricular administration of CNP-22 (4.5 nmol/mouse) and CNP-53 (1.5 nmol/mouse) on nocturnal food intake in mice. Food intake was observed for 15 h after intracerebroventricular injection. Data represent mean ± SEM. The number of mice is given in parentheses. Significant differences: *$P < 0.05$, **$P < 0.01$.**

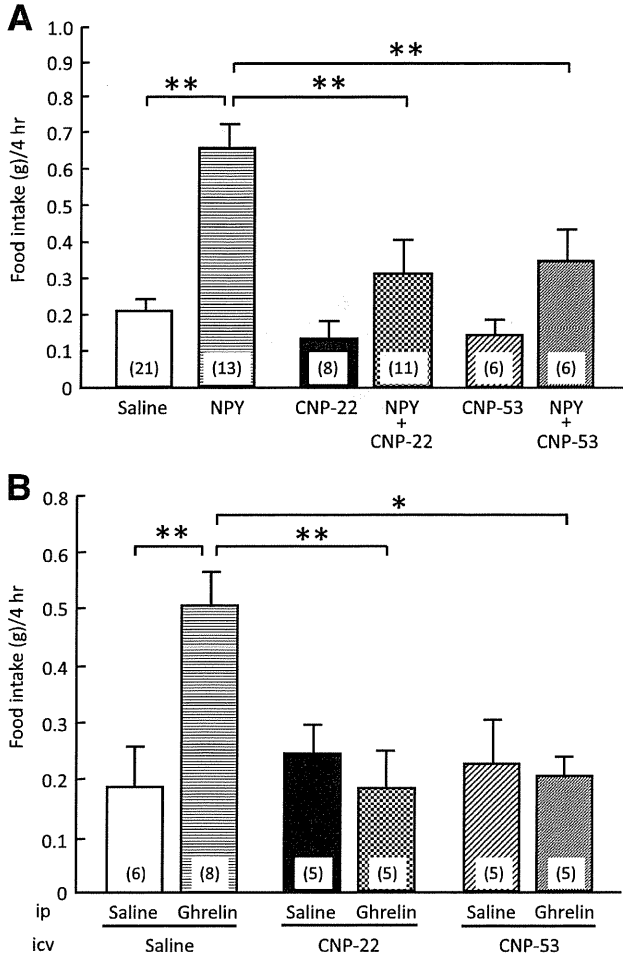


**FIG. 2. Effects of CNP-22 and CNP-53 on food intake induced by NPY and ghrelin. *A*: Effects of intracerebroventricular administration of CNP-22 (4.5 nmol/mouse) and CNP-53 (1.5 nmol/mouse) on NPY-induced (5 nmol/mouse, intracerebroventricular) food intake in mice. Food intake was observed for 4 h after coadministration of NPY and CNP. *B*: Effects of intracerebroventricular administration of CNP-22 (4.5 nmol/mouse) and CNP-53 (1.5 nmol/mouse) on ghrelin-induced (100 nmol/kg, intraperitoneal) food intake in mice. Food intake was observed for 4 h after coadministration of ghrelin and CNP. Data represent mean ± SEM. The number of mice is given in parentheses. Significant differences: *$P < 0.05$, **$P < 0.01$.**

**c-Fos–immunoreactive cells in the hypothalamus after intracerebroventricular administration of CNP.** To understand the neuronal pathway involved in the anorectic actions of CNP, the expression of c-Fos, one of the markers of neuronal activation, was monitored by immunohistochemical examination at 1 h after intracerebroventricular injection of CNP-53 (1.5 nmol/mouse). The numbers of c-Fos–immunoreactive cells in the ARC, PVN, and DMH were predominantly increased after intracerebroventricular injection of CNP-53 in comparison with saline treatment (Fig. 4*A*). The c-Fos–positive cells were also moderately increased in the VMH and LH (Fig. 4*A*). Next, we examined whether c-Fos immunoreactivity coexisted with α-MSH–containing cells. In the ARC of saline-treated mice, only a few α-MSH–immunoreactive cells showed weak c-Fos immunoreactivity (Fig. 4*B*). However, c-Fos–immunoreactive cells that increased with intracerebroventricular administration of CNP-53 in the ARC expressed a large amount of α-MSH immunoreactivity (Fig. 4*B*).

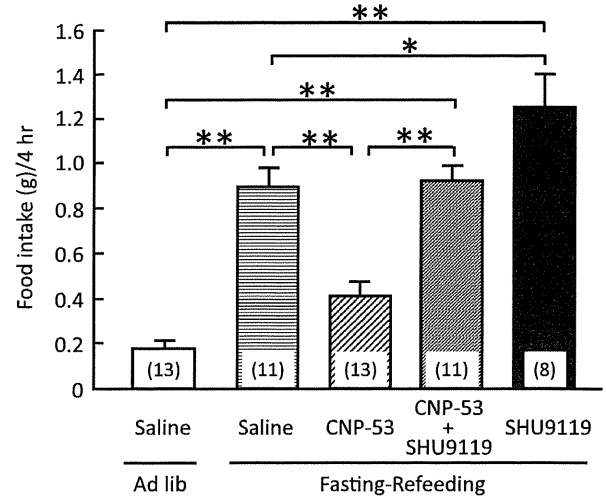


**FIG. 3. Effects of intracerebroventricular administration of CNP-53 (1.5 nmol/mouse) and SHU9119 (1 nmol/mouse) on refeeding after 48-h fasting in mice. Food intake was observed for 4 h after refeeding. Data represent mean ± SEM. The number of mice is given in parentheses. Significant differences: *$P < 0.05$, **$P < 0.01$.**

## DISCUSSION

The current study demonstrated that intracerebroventricular administration of CNP-22 and CNP-53, but not intraperitoneal injection, led to significant reduction of food intake induced by fasting–refeeding. This reduction was inhibited by the melanocortin-3 receptor (MC3R)/melanocortin-4 receptor (MC4R) antagonist SHU9119. In addition, CNP significantly suppressed nocturnal food intake and orexigenic actions induced by NPY and ghrelin. The immunohistochemical study revealed that intracerebroventricular administration of CNP-53 increased the number of c-Fos–expressing cells containing α-MSH in the hypothalamus. These findings indicated that the intracerebroventricular administration of CNP exhibits anorexigenic actions partially via activation of the melanocortin system, although the doses of CNP used in the current study could be pharmacological doses.

The hypothalamus is considered to be an important region in regulating energy homeostasis. In particular, the ARC in the hypothalamus contains both an orexigenic peptide, NPY, and an anorexigenic peptide, α-MSH, and is postulated to be involved in the first-order regulation of food intake. Synthetic MC3R/MC4R agonists, melanotan II, and [Nle$^4$-D-Phe$^7$]–α-MSH completely blocked food deprivation–induced increase in food intake as well as the food intake stimulated by intracerebroventricular administration of NPY (10,11). Regarding the reciprocal interactions of α-MSH and NPY, melanocortin neurons in the ARC project to the PVN (12). In the current study, intracerebroventricular administration of CNP significantly suppressed food intake after fasting, which was antagonized by SHU9119. Our results also showed that CNP suppressed NPY-induced food intake. Taken together, these findings indicate that CNP exhibits anorexigenic actions via activation of MC3R/MC4R downstream signaling. However, mRNA expressions of preopiomelanocortin, cocaine and amphetamine-related peptide, *NPY*, and *AgRP* in the hypothalamus after the intracerebroventricular injection of CNP-53 in fasting–refeeding experiment did not change compared with those after saline. The reason for this

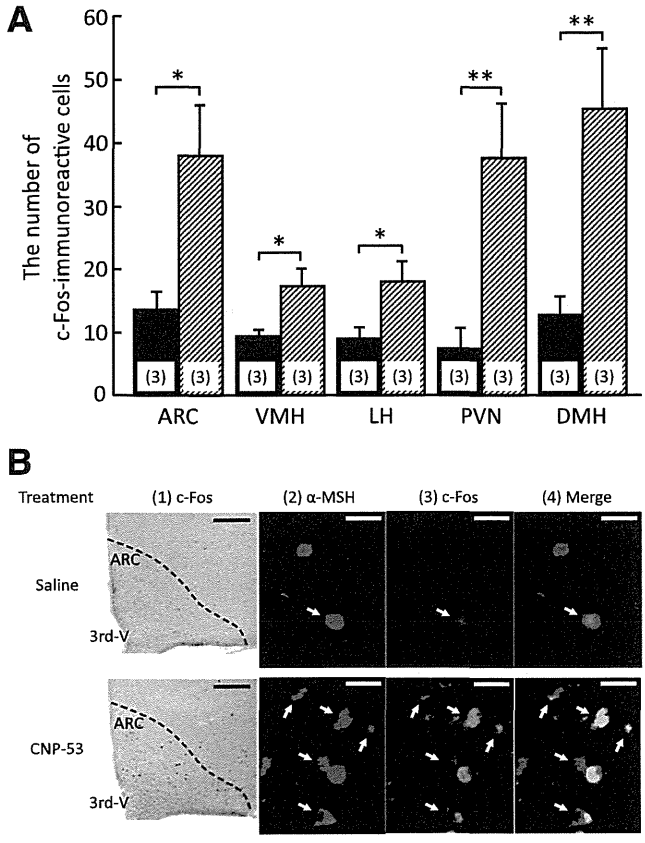


**FIG. 4. The c-Fos–immunoreactive cells in the hypothalamus after intracerebroventricular administration of CNP-53 (1.5 nmol/mouse). *A*: Number of c-Fos–immunoreactive cells after saline and CNP-53 treatments. Data represent mean ± SEM. The number of mice is given in parentheses. Significant differences: *$P < 0.05$, **$P < 0.01$. *B*: c-Fos–immunoreactive cells induced by intracerebroventricular administration of saline and CNP-53 (1). 3rd-V, the third ventricular. Scale bars, 100 μm. Coexistence of α-MSH (red) and c-Fos (green) immunoreactivity in the ARC (2–4) after saline (*upper*) and CNP-53 (1.5 nmol/mouse; *lower*) treatments. White arrows indicate cells expressing both α-MSH and c-Fos immunoreactivity. 3rd-V, the third ventricular. Scale bars, 20 μm.**

discrepancy may lie in the experimental condition, time course, and regional specificity. To clarify this discrepancy, further examinations will be required.

This study demonstrated that the intracerebroventricular administration of CNP significantly suppressed the nocturnal food intake. Robust feeding during the nocturnal phase of the daily light–dark cycle was demonstrated to be attributed to the upregulation of NPY and its receptors (13). These findings indicate that CNP may decrease food intake in the nocturnal phase via suppression of NPY action.

In the current study, CNP significantly suppressed the increase in food intake induced by ghrelin, an orexigenic hormone secreted by the stomach (14). NPR-B, a CNP receptor, has been identified in appetite-regulating regions, such as the ARC, VMH, PVN, DMH, and LH (15). The systemic administration of ghrelin significantly increased NPY and AgRP expression in the ARC of the hypothalamus in fed and fasted rats (15), resulting in hyperphagia. The intracerebroventricular injection of melanotan II caused a significant decrease in ghrelin-induced food intake (16). These findings suggest that the actions of ghrelin are modulated by α-MSH and NPY systems. Furthermore, plasma ghrelin and hypothalamic ghrelin receptor mRNA expression are reported to be increased after fasting (17,18). These findings suggest the possibility that intracerebroventricular administration of CNP activates the melanocortin system, which subsequently inhibits the action of NPY, resulting in a reduced increase of food intake induced by ghrelin.

To assess which hypothalamic nucleus is involved in the anorexigenic action of CNP, a marker for neuronal activity, c-Fos expression in the hypothalamus was examined after intracerebroventricular administration of CNP-53. The intracerebroventricular administration of CNP-53 significantly increased the number of c-Fos–expressing cells in several hypothalamic nuclei, such as ARC, PVN, DMH, VMH, and LH, indicating that CNP-53 directly or indirectly stimulates neurons in these hypothalamic nuclei. Especially in the ARC, the result was an increased number of c-Fos–immunoreactive cells containing α-MSH immunoreactivity, indicating that CNP stimulates α-MSH–containing neurons. This possibility is supported by the finding that the suppressive action of CNP-53 on food intake was blocked by concomitant administration of SHU9119, an MC3R/MC4R antagonist.

The current study has demonstrated the anorexigenic action of intracerebroventricular administration of CNP via activation of the melanocortin system. To define the precise effect of CNP in the brain on food intake, further investigation using mice with inducible brain-specific deletion of CNP or NPR-B/NPR-C will be required.

From the present findings, we postulate the possible mechanism for anorexigenic action of exogenous CNP to be as follows: CNP directly or indirectly acts on α-MSH–containing neurons and subsequently stimulates α-MSH release, resulting in suppression of food intake induced by NPY and ghrelin. This possible mechanism may apply to the suppressive effects of CNP on food intake after fasting and in the nocturnal phase. Further work is needed to define the pathophysiological significance of brain CNP in regulation of food intake.

## ACKNOWLEDGMENTS

This work was supported in part by research grants from the Ministry of Education, Culture, Sports, Science, and Technology of Japan, and the Ministry of Health, Labour, and Welfare of Japan.

No potential conflicts of interest relevant to this article were reported.

N.Y.-G. and G.K. performed experiments, contributed to discussion, and wrote the manuscript. K.E., M.I., Y.O., Y.Y., T.K., A.Y., N.S.-A., H.A., and K.H. contributed to discussion. K.N. contributed to discussion, and reviewed and edited the manuscript. K.N. is the guarantor of this work and, as such, had full access to all the data in the study and takes responsibility for the integrity of the data and the accuracy of the data analysis.

## REFERENCES

1. Minamino N, Makino Y, Tateyama H, Kangawa K, Matsuo H. Characterization of immunoreactive human C-type natriuretic peptide in brain and heart. Biochem Biophys Res Commun 1991;179:535–542
2. Herman JP, Langub MC Jr, Watson RE Jr. Localization of C-type natriuretic peptide mRNA in rat hypothalamus. Endocrinology 1993;133:1903–1906
3. Langub MC Jr, Watson RE Jr, Herman JP. Distribution of natriuretic peptide precursor mRNAs in the rat brain. J Comp Neurol 1995;356:183–199
4. Langub MC Jr, Dolgas CM, Watson RE Jr, Herman JP. The C-type natriuretic peptide receptor is the predominant natriuretic peptide receptor mRNA expressed in rat hypothalamus. J Neuroendocrinol 1995;7:305–309

5. Herman JP, Dolgas CM, Rucker D, Langub MC Jr. Localization of natriuretic peptide-activated guanylate cyclase mRNAs in the rat brain. J Comp Neurol 1996;369:165-187
6. Yamada N, Katsuura G, Ochi Y, Ebihara K, Kusakabe T, Hosoda K, Nakao K. Impaired CNS leptin action is implicated in depression associated with obesity. Endocrinology 2011;152:2634–2643
7. Nakao K, Katsuura G, Morii N, Itoh H, Shiono S, Yamada T, Sugawara A, Sakamoto M, Saito Y, Eigyo M, Matsushita A, Imura H. Inhibitory effect of centrally administered atrial natriuretic polypeptide on the brain dopaminergic system in rats. Eur J Pharmacol 1986;131:171–177
8. Yamada N, Katsuura G, Tatsuno I, et al. Orexin decreases mRNA expressions of NMDA and AMPA receptor subunits in rat primary neuron cultures. Peptides 2008;29:1582–1587
9. Paxinos G, Franklin KBJ. *The mouse brain in stereotaxic coordinates.* New York, Academic Press, 2004
10. Brown KS, Gentry RM, Rowland NE. Central injection in rats of alpha-melanocyte-stimulating hormone analog: effects on food intake and brain Fos. Regul Pept 1998;78:89–94
11. Murphy B, Nunes CN, Ronan JJ, et al. Melanocortin mediated inhibition of feeding behavior in rats. Neuropeptides 1998;32:491–497
12. Sánchez E, Singru PS, Acharya R, et al. Differential effects of refeeding on melanocortin-responsive neurons in the hypothalamic paraventricular nucleus. Endocrinology 2008;149:4329–4335
13. Kalra PS, Dube MG, Xu B, Farmerie WG, Kalra SP. Evidence that dark-phase hyperphagia induced by neurotoxin 6-hydroxydopamine may be due to decreased leptin and increased neuropeptide Y signaling. Physiol Behav 1998;63:829–835
14. Kojima M, Hosoda H, Date Y, Nakazato M, Matsuo H, Kangawa K. Ghrelin is a growth-hormone-releasing acylated peptide from stomach. Nature 1999;402:656–660
15. Harrold JA, Dovey T, Cai XJ, Halford JC, Pinkney J. Autoradiographic analysis of ghrelin receptors in the rat hypothalamus. Brain Res 2008;1196:59–64
16. Shrestha YB, Wickwire K, Giraudo SQ. Action of MT-II on ghrelin-induced feeding in the paraventricular nucleus of the hypothalamus. Neuroreport 2004;15:1365–1367
17. Keen-Rhinehart E, Bartness TJ. NPY Y1 receptor is involved in ghrelin- and fasting-induced increases in foraging, food hoarding, and food intake. Am J Physiol Regul Integr Comp Physiol 2007;292:R1728–R1737
18. Kim MS, Yoon CY, Park KH, et al. Changes in ghrelin and ghrelin receptor expression according to feeding status. Neuroreport 2003;14:1317–1320

  

METABOLISM CLINICAL AND EXPERIMENTAL 62 (2013) 70–78

Available online at www.sciencedirect.com

Metabolism

www.metabolismjournal.com

# GPR119 expression in normal human tissues and islet cell tumors: evidence for its islet-gastrointestinal distribution, expression in pancreatic beta and alpha cells, and involvement in islet function

*Shinji Odori*[a], *Kiminori Hosoda*[a,*], *Tsutomu Tomita*[a], *Junji Fujikura*[a], *Toru Kusakabe*[a], *Yoshiya Kawaguchi*[b], *Ryuichiro Doi*[b], *Kyoichi Takaori*[b], *Ken Ebihara*[a], *Yoshiharu Sakai*[b], *Shinji Uemoto*[b], *Kazuwa Nakao*[a]

[a] *Department of Medicine and Clinical Science, Kyoto University Graduate School of Medicine, 54 Shogoin Kawahara-cho, Sakyo-ku, Kyoto 606–8507, Japan*

[b] *Department of Surgery, Kyoto University Graduate School of Medicine, 54 Shogoin Kawahara-cho, Sakyo-ku, Kyoto 606–8507, Japan*

ARTICLE INFO

*Article history:*
Received 25 April 2012
Accepted 27 June 2012

*Keywords:*
Insulinoma
Glucagonoma
Insulin secretion
Gastrointestinal hormones

ABSTRACT

*Objective.* GPR119 is reportedly involved in regulating glucose metabolism and food intake in rodents, but little is known about its expression and functional significance in humans. To begin to assess the potential clinical importance of GPR119, the distribution of *GPR119* gene expression in humans was examined.

*Materials/Methods.* Expression of GPR119 mRNA in fresh samples of normal human pancreas ($n=19$) and pancreatic islets ($n=3$) and in insulinomas ($n=2$) and glucagonomas ($n=2$), all collected at surgery, was compared with the mRNA expression of various receptors highly expressed and operative in human pancreatic islets.

*Results.* GPR119 mRNA was most abundant in the pancreas, followed by the duodenum, stomach, jejunum, ileum and colon. Pancreatic levels of GPR119 mRNA were similar to those of GPR40 mRNA and were higher than those of GLP1R and SUR1 mRNA, which are strongly expressed in human pancreatic islets. Moreover, levels of GPR119 mRNA in pancreatic islets were more than 10 times higher than in adjacent pancreatic tissue, as were levels of GPR40 mRNA. GPR119 mRNA was also abundant in two cases of insulinoma and two cases of glucagonoma, but was undetectable in a pancreatic acinar cell tumor. Similar results were obtained with mouse pancreatic islets, MIN6 insulinoma cells and alpha-TC glucagonoma cells.

*Conclusions.* The results provide evidence of an islet-gastrointestinal distribution of GPR119, its expression in pancreatic beta and alpha cells, and its possible involvement in islet function. They also provide the basis for a better understanding of the potential clinical importance of GPR119.



*Abbreviations:* FFPE, formalin-fixed, paraffin-embedded; GLP1R, glucagon-like peptide 1 receptor; GPR119, G protein-coupled receptor 119; GPR40, G protein-coupled receptor 40; SUR1, sulfonylurea receptor 1.

* *Corresponding author.* Tel.: +81 75 751 3172; fax: +81 75 771 9452.
E-mail address: kh@kuhp.kyoto-u.ac.jp (K. Hosoda).

0026-0495/$ – see front matter © 2013 Elsevier Inc. All rights reserved.
http://dx.doi.org/10.1016/j.metabol.2012.06.010

## 1. Introduction

Endogenous lipids such as free fatty acids and acylethanolamides are known to regulate glucose metabolism and food intake [1–3]. The underlying molecular mechanisms are not fully understood, however. Recently, four orphan G protein-coupled receptors (GPR40, GPR41, GPR43 and GPR120) were deorphaned and identified as fatty acid receptors [4–8]. Among those, we found that GPR40 is highly expressed in human pancreatic beta cells and is involved in regulating insulin secretion [9,10]. In addition, GPR119 has been identified as a Gs-coupled receptor whose putative endogenous ligands include oleoylethanolamide (OEA) [11,12] and possibly other lipids [13–16]. *In vitro* studies have implicated GPR119 in the regulation of insulin and incretin secretion [12,14,15,17–20], and *in vivo* studies in rats and mice suggest its involvement in the regulation of glucose metabolism and feeding [11,14,18,19,21–30]. That said, glucose metabolism in humans and mice may differ [31], and little is known about the expression and physiological significance of GPR119 in humans.

In that context, we examined *GPR119* gene expression in various human tissues, including fresh samples of pancreas and digestive tract collected at surgery. In addition, to gain further insight into the localization of GPR119 within the human pancreas, we compared *GPR119* expression in human pancreatic islets and adjacent pancreatic tissue, as well as in insulinomas and glucagonomas, two very rare human tumors that possess the endocrine properties of pancreatic beta and alpha cells, respectively. The results provide evidence of the islet-gastrointestinal distribution of GPR119, its expression in pancreatic beta and alpha cells, and its possible involvement in islet function in humans.

**Table 1 – Clinical profiles of the patients who underwent pancreatectomy and tissues analyzed.**

| Patient | Age (years) | Sex (M/F) | Disease | Tissue analyzed |
|---|---|---|---|---|
| 1 | 26 | M | Pancreatic cancer | Pancreas (tail) |
| 2 | 47 | F | Pancreatic cancer | Pancreas (head) |
| 3 | 53 | F | Pancreatic cancer | Pancreas (head) |
| 4 | 54 | M | Pancreatic cancer | Pancreas (head) |
| 5 | 55 | F | Pancreatic cancer | Pancreas (body) |
| 6 | 57 | M | Islet cell tumor (nonfunctional) | Pancreas (tail) |
| 7 | 59 | F | Insulinoma | Pancreas (head), insulinoma |
| 8 | 60 | M | Pancreatic cancer | Pancreas (body) |
| 9 | 60 | M | Pancreatic cancer | Pancreas (head) |
| 10 | 61 | F | Papilla cancer | Pancreas (head) |
| 11 | 63 | F | Islet cell tumor (nonfunctional) | Pancreas (body) |
| 12 | 63 | M | Pancreatic cancer | Pancreas (head) |
| 13 | 64 | M | Pancreatic cancer | Pancreas (body) |
| 14 | 69 | M | Pancreatic cancer | Pancreas (head) |
| 15 | 71 | F | Pancreatic cancer | Pancreas (body) |
| 16 | 72 | F | Pancreatic cancer | Pancreas (body) |
| 17 | 72 | F | Pancreatic cancer | Pancreas (head) |
| 18 | 75 | M | Pancreatic cancer | Pancreas (head) |
| 19 | 76 | M | Duodenal cancer | Pancreas (head) |
| 20 | 27 | F | Insulinoma | Insulinoma |
| 21 | 23 | F | Glucagonoma | Glucagonoma |
| 22 | 41 | F | Acinar cell tumor | Acinar cell tumor |
| 23 | 34 | F | Glucagonoma | Glucagonoma |

Patients were premedicated with 0.01 mg/kg atropine sulfate i.m. and 0.2 mg/kg diazepam orally before surgery. Tissues were sampled under general anesthesia with 35% $O_2$, 65% $N_2O$ and 0.5%–1.5% sevoflurane. Neuromuscular blockade was provided by vecuronium bromide at an initial dose 0.1 mg/kg and supplemented as required.

## 2. Methods

### 2.1. *Subjects, tissue sampling and pancreatic islet isolation*

The clinical profiles of all patients enrolled in the present study are shown in Table 1. The study was performed in accordance with the Declaration of Helsinki and approved by the Ethical Committee on Human Research of Kyoto University Graduate School of Medicine. Signed informed consent was obtained from all patients.

Normal human cerebral tissues ($n=3$) were collected from three patients at autopsy; one had died from amyotrophic lateral sclerosis, one from an iliopsoas muscle tumor and one from a ruptured aortic aneurysm. Normal tissues from the pancreas ($n=19$), esophagus ($n=3$), stomach ($n=3$), duodenum ($n=3$), jejunum ($n=3$), ileum ($n=2$), colon ($n=3$) and liver ($n=2$) were collected from 23 patients at tumor resection. In Fig. 1B and C, pancreatic tissues from four patients (patients 9, 10, 13 and 19 in Tables 1 and 2) were analyzed because of the limited amount of total RNA extracted from each patient. In all cases, sample margins contained no sign of tumor invasion, so the samples were considered to be tumor-free. In addition, samples of insulinoma ($n=2$), glucagonoma ($n=1$) and a pancreatic acinar cell tumor ($n=1$) were collected at surgery. From another patient with a glucagonoma, samples of normal pancreatic tissue and glucagonoma were obtained as formalin-fixed, paraffin-embedded (FFPE) sections. Islets were promptly isolated from pancreatic samples using the mince method and were collected manually using a stereomicroscope [9,10]. In Japan, HbA1c is measured using high-performance liquid chromatography with a set of calibrators assigned by the Japan Diabetes Society (normal range 4.3%–5.8%). A correlational analysis showed that, in Japan, estimated HbA1c values are 0.4% lower than those measured by the National Glycohemoglobin Standardization Program (NGSP) [32]. For that reason, we standardized the obtained HbA1c values to NGSP units by adding 0.4% to the measured values.

### 2.2. *Preparation and culture of mouse pancreatic islets, the MIN6 mouse insulinoma cell line and the alpha-TC mouse glucagonoma cell line*

Male 14-week-old C57BL/6 mice were purchased from Japan SLC (Shizuoka, Japan) and housed in a temperature-, humidity- and light-controlled room with free access to water and standard chow (Nosan, Kanagawa, Japan). Mouse pancreatic islets were isolated as previously described [33]. All experimental procedures were approved by the Animal Research

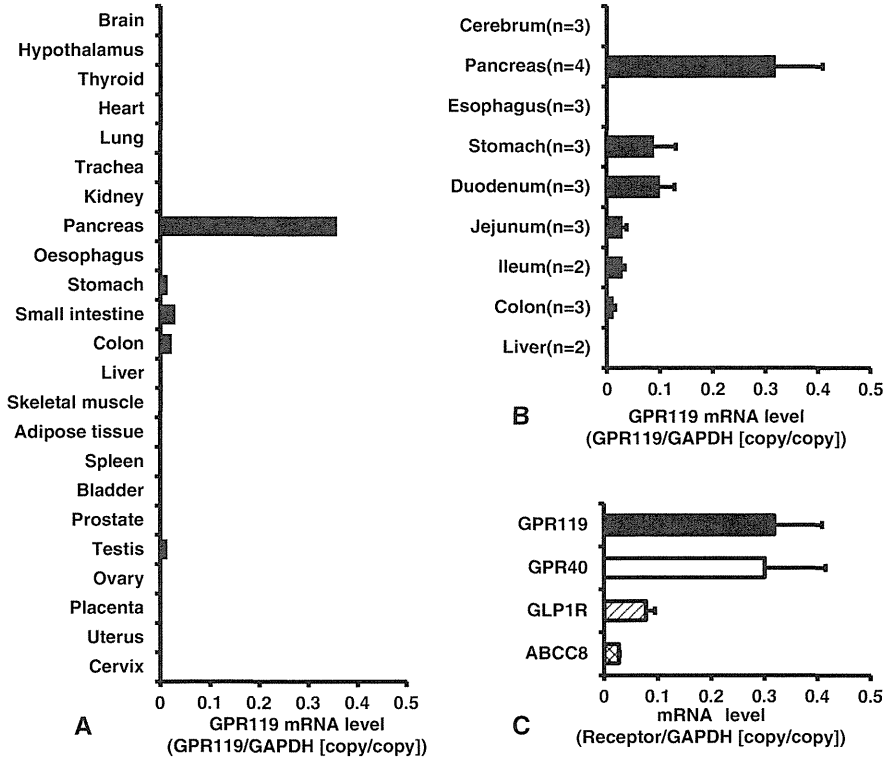


**Fig. 1 – Expression of GPR119 mRNA in human tissues. All receptor mRNA levels were normalized to the level of GAPDH mRNA in the same tissue. A, GPR119 mRNA levels in commercially obtained samples of human total RNA from the indicated tissues. B, GPR119 mRNA expression in the indicated human tissues collected at autopsy (cerebrum) or at surgery (all tissues except cerebrum). C, Expression of GPR119, GPR40, GLP1R and SUR1 mRNA in normal human pancreatic tissue collected at surgery ($n=4$). The specimens used were the same as in panel B. Receptor mRNA levels in panels B and C are expressed as means ± SEM. *Black bar*, GPR119; *white bar*, GPR40; *hatched bar*, GLP1R; *double-hatched bar*, ABCC8 (SUR1).**

**Table 2 – The metabolic parameters and the levels of GPR119 mRNA in the pancreas of 19 patients.**

| Patient | BMI ($kg/m^2$) | FPG (mmol/L) | 2 h-PG (mmol/L) | Insulin AUC ($\times 10^3$ pmol/L) | HbA1c (%) | HOMA-IR | Insulinogenic index | HOMA-beta | Triglycerides (mmol/L) | GPR119 mRNA level |
|---|---|---|---|---|---|---|---|---|---|---|
| 1 | 24.2 | 4.7 | 6.7 | 32 | 5.1 | 9.6 | 83.0 | 124.4 | 1.23 | 0.183 |
| 2 | 19.7 | 7.2 | 12.6 | 53 | 7.1 | 36.6 | 100.1 | 102.1 | 2.26 | 0.334 |
| 3 | 17.7 | 4.4 | 6.8 | 24 | 5.1 | 2.8 | 62.7 | 50.8 | 1.54 | 0.430 |
| 4 | 22.3 | 4.9 | 9.1 | 18 | 5.7 | 3.7 | 17.8 | 40.3 | 0.89 | 0.112 |
| 5 | 24.6 | 5.1 | 8.3 | 25 | 5.1 | 5.7 | 42.8 | 54.0 | 1.20 | 0.235 |
| 6 | 25.7 | 6.1 | *ND* | *ND* | 5.6 | 24.0 | *ND* | 112.60 | 1.48 | 0.342 |
| 7* | 22.1 | 2.0 | 4.9 | 84 | 4.7 | 2.5 | *ND* | −61.3 | 0.86 | 0.419 |
| 8 | 18.0 | 5.3 | 10.8 | 12 | 6.3 | 3.3 | 23.6 | 25.1 | 1.76 | 0.063 |
| 9 | 19.6 | 4.3 | 11.4 | *ND* | 5.4 | 2.0 | *ND* | 40.8 | 2.01 | 0.228 |
| 10 | 20.0 | 4.6 | 6.9 | 24 | 5.0 | 8.4 | 163.7 | 130.7 | 1.40 | 0.583 |
| 11 | 22.8 | 5.5 | 13.6 | *ND* | 6.7 | 8.5 | *ND* | 58.0 | 2.28 | 0.483 |
| 12† | 24.2 | 4.8 | *ND* | *ND* | 6.5 | *ND* | *ND* | *ND* | 1.01 | 0.582 |
| 13 | 23.3 | 5.2 | 10.7 | 18 | 5.8 | 8.5 | 11.1 | 70.8 | 1.29 | 0.185 |
| 14 | 24.3 | *ND* | *ND* | *ND* | 7.1 | *ND* | *ND* | *ND* | 0.95 | 0.272 |
| 15 | 23.5 | 4.9 | 8.9 | *ND* | 6.2 | 10.3 | *ND* | 113.8 | 1.99 | 0.492 |
| 16 | 18.4 | 6.1 | *ND* | *ND* | 6.5 | *ND* | *ND* | *ND* | 2.03 | 0.306 |
| 17† | 16.8 | 5.1 | *ND* | *ND* | 5.8 | *ND* | *ND* | *ND* | 1.02 | 0.631 |
| 18 | 22.6 | 5.4 | 8.3 | 51 | 6.2 | 6.8 | 47.8 | 48.3 | 1.60 | 0.219 |
| 19 | 20.3 | 4.2 | 6.8 | 48 | 5.4 | 3.0 | 103.1 | 81.0 | 0.49 | 0.279 |

The patient numbers correspond to those in Table 1. *Patient 7 was diagnosed as having an insulinoma. †Patients 12 and 17 were treated with percutaneous transhepatic biliary drainage (PTBD). Because of the unavailability of blood samples, some of the metabolic profiles were not determined (shown as *ND*). *FPG*, fasting plasma glucose level; *2 h-PG*, 2-h post-OGTT plasma glucose level; *ND*, not determined.

Committee, Kyoto University Graduate School of Medicine, and were performed in accordance with institutional and national guidelines for animal experimentation. MIN6 cells were kindly provided by Dr. Junichi Miyazaki [34], and alpha-TC cells were obtained from American Type Culture Collection (ATCC) (Manassas, VA, USA). MIN6 cells were maintained in Dulbecco's modified Eagle's medium supplemented with 15% FBS, while alpha-TC cells were maintained in RPMI 1640 medium supplemented with 10% FBS. Both media also contained 100 U/mL penicillin and 0.1 mg/mL streptomycin (Life Technologies Japan, Tokyo, Japan). The cells were incubated at 37 °C under an atmosphere of humidified air (95%) and $CO_2$ (5%).

### 2.3. *Total RNA preparation and cDNA synthesis*

Total RNAs were extracted from fresh tissues and cell lines using QIAGEN RNeasy Mini Kits [9,10,33], and from FFPE tissue sections using QIAGEN RNeasy FFPE Kits (QIAGEN K.K., Tokyo, Japan). The collected RNA was then treated with DNase I to remove any contaminating DNA. Additionally, total RNAs from human brain, thyroid, heart, lung, trachea, kidney, esophagus, liver, skeletal muscle, adipose tissue, spleen, bladder, prostate, placenta and cervix were obtained from Life Technologies Japan. Total RNAs from stomach, small intestine, colon, pancreas, testis, ovary and uterus were from Takara Clontech (Tokyo, Japan). Finally, total RNAs from hypothalamus were obtained from two sources, Life Technologies Japan and BioChain Institute (Hayward, CA, USA). First strand cDNA was synthesized by random hexamer-primed reverse transcription using SuperScript II reverse transcriptase (Life Technologies Japan).

### 2.4. *Quantification of human and mouse receptor gene expression*

Levels of GPR119 mRNA in the pancreas and pancreatic islets were compared with those of GPR40, the glucagon-like peptide-1 receptor (GLP1R) and the sulfonylurea receptor 1 (ABCC8 or SUR1) mRNA, which are reportedly expressed in human pancreatic islets and involved in insulin secretion [9,10]. Messenger RNA levels were quantified using the TaqMan PCR method with an ABI PRISM 7700 Sequence Detector (Life Technologies Japan), as described previously [9,10]. To estimate the copy number of each mRNA, standard curves were generated using oligo DNA fragments (Sigma Genosys Japan, Tokyo, Japan) containing the PCR amplicon region. The receptor mRNA levels were normalized to the level of GAPDH mRNA and expressed as the receptor/GAPDH [copy/copy] ratio [9]. The sequences of the primers and probes (Life Technologies Japan) used for the quantification of the mRNAs were as follows: human *GPR119* (NM_178471), CCATGGCTGGAGGTTATCGA (forward), GCTCCCAATGAGAACA-GACACA (reverse) and 6-carboxyfluorescein (FAM)-CCCCACG-GACTCCCAGCGACT-6-carboxytetramethylrhodamine (TAMRA) (probe); mouse *GPR119* (NM_181751), TCCAGAGAGGACCAGA-GAAAGC (forward), GCAGCGTCTTAGCCATCGA (reverse) and FAM-TCACATCGTCACTATCAGCCATCCGG-TAMRA (probe); mouse *GPR40* (NM_194057), GGCTTTCCATTGAACTTGTTAGC (forward), CCCAGATGGAGAGTGTAGACCAA (reverse) and FAM-TGTCCCACGCTAAACTGCGACTCACTC-TAMRA (probe); mouse *GADPH* (NM_008084), TCCATGCCATCACTGCCA (forward), GCCCCACGGCCATCA (reverse) and FAM-CAGAAGACTGTG-GATGGCCCCTC-TAMRA (probe). The sequences of the primers and probes used for quantification of the human GPR40, GLP1R, ABCC8 (SUR1) and GAPDH mRNAs are described elsewhere [9,10].

### 2.5. *Data analysis on metabolic parameters*

We evaluated beta cell function and systemic insulin resistance using the insulinogenic index ($n=10$) [35] or the homeostasis model assessment of beta cell function (HOMA-beta) ($n=14$) and insulin resistance (HOMA-IR) ($n=14$) [36], respectively. The difference between the numbers of patients whose test data were included in the HOMA indices and insulinogenic index reflects the availability of data for plasma glucose and serum insulin levels at the 30 min mark during the oral glucose tolerance test (OGTT). The area under the serum insulin concentration–time curve (insulin AUC) was calculated from the OGTT data using the trapezoidal rule. Patients 7, 12 and 17 were excluded from analysis of the correlation between pancreatic GPR119 mRNA levels and metabolic parameters, because of a diagnosis of insulinoma (patient 7) or percutaneous transhepatic biliary drainage (patients 12 and 17). None of the patients were treated with oral glucose-lowering agents or with insulin. Table 2 shows the metabolic parameters of the patients whose pancreatic tissues were examined; the patient numbers correspond to those in Table 1.

### 2.6. *Statistical analysis*

Correlations between pancreatic GPR119 mRNA levels and clinical parameters were examined using the simple regression analysis. Differences between groups were assessed using unpaired two-tailed t tests or ANOVA where applicable. Values of $P<.05$ were considered significant (Statcel, Social Research Information, Tokyo, Japan).

## 3. Results

### 3.1. *Expression of GPR119 mRNA in normal human tissues*

We initially tested for GPR119 mRNA in samples of commercially available total RNA from normal human tissues. We found that the transcript was most abundant in the pancreas, followed by the gastrointestinal tract (small intestine, colon and stomach) and the testis (Fig. 1A). GPR119 mRNA was not detected in any other human tissue tested. To gain further insight into *GPR119* gene expression humans and verify the aforementioned distribution profile, we also examined tissues obtained at surgery or autopsy. Among those samples, GPR119 mRNA was most abundant in the pancreas, followed by the duodenum, stomach, jejunum, ileum and colon, but was not detected in the esophagus, liver or cerebrum (Fig. 1B).

### 3.2. *Expression of GPR119, GPR40, GLP1R and SUR1 mRNAs in the human pancreas*

Using specimens from four patients, we compared the pancreatic expression of GPR119 mRNA with that of GPR40,

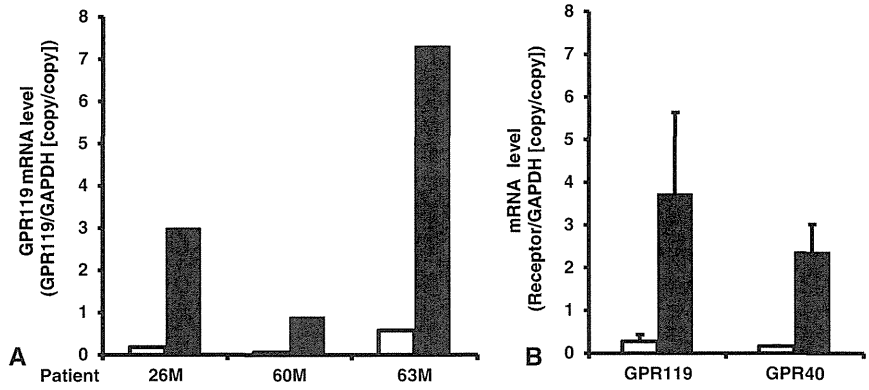


**Fig. 2 – Expression of GPR119 mRNA in human pancreatic islets and adjacent pancreatic tissue. All receptor mRNA levels were normalized to the level of GAPDH mRNA in the same tissue. A, Comparison of GPR119 mRNA expression in pancreatic islets and adjacent pancreatic tissue from three patients. *White bars*, pancreas; *black bars*, pancreatic islets. B, Comparison of GPR119 and GPR40 mRNA expression in pancreatic islets and adjacent pancreatic tissue. The tissue samples used were the same as in panel A ($n=3$). Levels of GPR119 and GPR40 mRNA are expressed as means ± SEM. *White bars*, pancreas; *black bars*, pancreatic islets.**

GLP1R and SUR1 mRNA in the same samples. We found that pancreatic levels of GPR119 mRNA were comparable to those of GPR40 mRNA and were higher than those of GLP1R and SUR1 mRNA (Fig. 1 C).

### 3.3. *Expression of GPR119 and GPR40 mRNA in isolated pancreatic islets and adjacent pancreatic tissue*

We next assessed GPR119 expression in pancreatic islets from three patients (Fig. 2A). Levels of GPR119 mRNA in freshly isolated islets were approximately 13 to 16 times higher than in the adjacent pancreatic tissue from the same patients. We also analyzed GPR40 expression and found that levels of GPR119 and GPR40 mRNA were similar in isolated pancreatic islets (Fig. 2B).

### 3.4. *Expression of GPR119 and GPR40 mRNA in human insulinomas and glucagonomas*

We also assessed expression of GPR119 and GPR40 mRNA using total RNAs extracted from specimens of fresh insulinomas ($n=2$), a glucagonoma ($n=1$) and a pancreatic acinar cell tumor ($n=1$), as well as from FFPE glucagonoma tissue sections from another patient ($n=1$). In the two cases of insulinoma, tumoral GPR119 mRNA levels were comparable to those in pancreatic islets (Fig. 3A). A considerable amount of GPR119 mRNA was also detected in tissue extracts from the glucagonoma (Fig. 3A), where GPR40 mRNA was not detectable (Fig. 3 C). Levels of GPR119 mRNA in tissue extracts from FFPE sections of non-tumor pancreas and glucagonoma were similar to those in the corresponding specimens collected at surgery (Fig. 3, A and B). GPR40 mRNA was not detected in extracts from the same FFPE glucagonoma sections (Fig. 3D), which is consistent with the level in the fresh tumor specimen (Fig. 3, C and D). Neither GPR119 nor GPR40 mRNAs was detectable in the acinar cell tumor specimen (Fig. 3, A and C).

### 3.5. *Expression of GPR119 and GPR40 mRNAs in mouse pancreatic islets, MIN6 insulinoma cells and alpha-TC glucagonoma cells*

To further explore GPR119 expression in pancreatic islet cells, we measured GPR119 mRNA levels in mouse pancreatic islets, MIN6 insulinoma cells and alpha-TC glucagonoma cells. We also assessed expression of GPR40 mRNA in the same samples, as GPR40 is known to be preferentially expressed in pancreatic beta cells in both rodents and humans [4,9,10,37]. High levels of GPR119 mRNA, comparable to those of GPR40 mRNA, were detected in mouse pancreatic islets (Fig. 4, A and B). Likewise, similar levels of GPR119 and GPR40 mRNA were detected in MIN6 cells (Fig. 4, A and B). On the other hand, the level of GPR119 mRNA in alpha-TC cells was approximately 1/7 that in MIN6 cells, and no GPR40 mRNA was detected in alpha-TC cells (Fig. 4, A and B).

### 3.6. *Correlation between pancreatic GPR119 mRNA expression and the insulinogenic index and HOMA-beta in humans*

To investigate the functional implications of pancreatic GPR119 expression in humans, we initially assessed GPR119 mRNA expression in non-tumor pancreatic tissue samples from 19 patients with various pancreatic tumors (Table 1). High levels of GPR119 mRNA, comparable to those in the four cases summarized in Fig. 1, A and B ($0.336 \pm 0.037$ vs $0.319 \pm 0.090$), were detected in all of the tissue samples analyzed (Table 2). Because the inter-individual variation in the pancreatic GPR119 mRNA level ($n=19$) was high, to begin to explore the physiological importance of GPR119 in humans, we evaluated the relationship between pancreatic GPR119 mRNA levels and various clinical parameters. We found that GPR119 mRNA expression did not significantly differ among the head, body and tail portions of the pancreas (Table 3), nor did it correlate significantly with age (Supplemental Table S1).

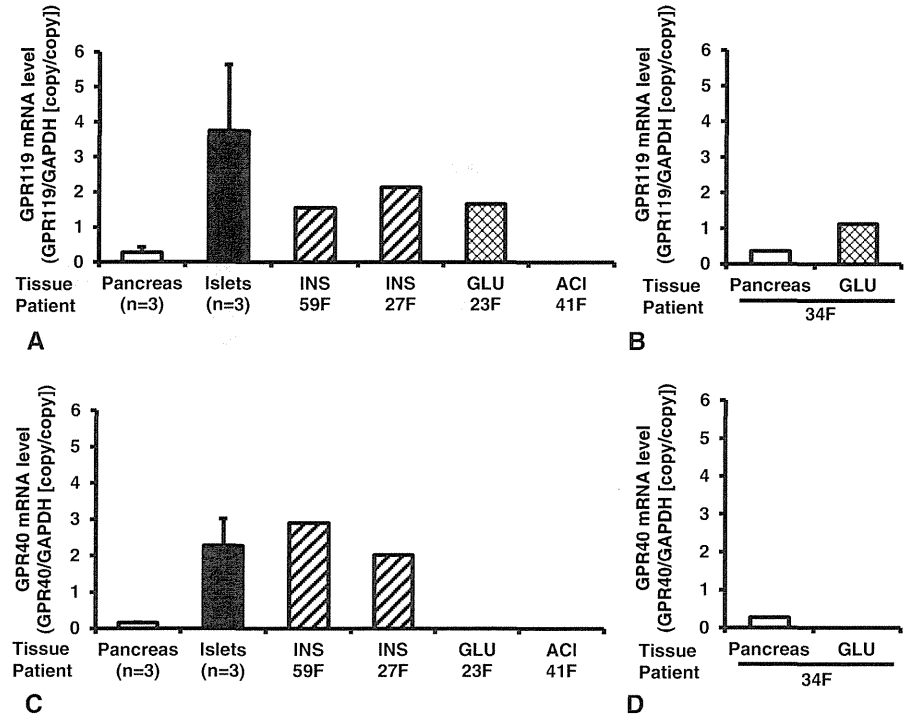


**Fig. 3 – Expression of GPR119 and GPR40 mRNA in human pancreatic islets, insulinomas and glucagonomas. A and C, Expression of GPR119 (A) and GPR40 (C) mRNA in non-tumor pancreas (Pancreas), pancreatic islets (Islets), insulinomas (INS), a glucagonoma (GLU) and a pancreatic acinar cell tumor (ACI). B and D, Expression of GPR119 (B) and GPR40 (D) mRNA in extracts from non-tumor pancreatic and glucagonoma tissue sections ($n=1$ each). All receptor mRNA levels were normalized to the level of GAPDH mRNA in the same tissue. GPR119 and GPR40 mRNA levels in pancreas and pancreatic islets are expressed as means ±SEM. *White bars*, pancreas; *black bars*, pancreatic islets; *hatched bars*, insulinomas; *double-hatched bars*, glucagonomas.**

When we then evaluated the correlation between pancreatic *GPR119* gene expression and several metabolic parameters, including glucose and triglyceride metabolism (Table 2), we found that pancreatic GPR119 mRNA levels did not correlate significantly with BMI, fasting plasma glucose (FPG), 2-h post-OGTT plasma glucose (2 h-PG), insulin AUC or fasting serum triglyceride levels (Supplemental Table S1), nor did they correlate significantly with HbA1c levels or HOMA-IR values (Supplemental Table S1, Fig. 5, A and B). By contrast, pancreatic GPR119 mRNA levels positively and significantly correlated with the insulinogenic index ($n=10$, $P=.004$, $r=0.817$) (Fig. 5 C) and with HOMA-beta values ($n=14$, $P=.043$, $r=0.547$) (Fig. 5D). Using the same patient data used to calculate the insulinogenic index ($n=10$) and HOMA-beta ($n=14$), we also tested for correlations

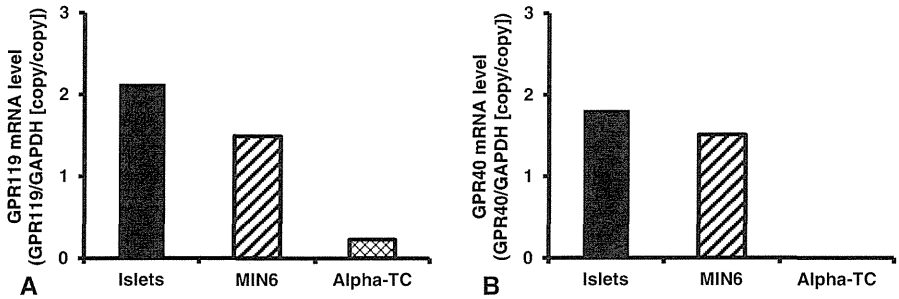


**Fig. 4 – Expression of GPR119 and GPR40 mRNAs in mouse pancreatic islets, insulinoma and glucagonoma. Expression of GPR119 (A) and GPR40 (B) mRNAs pancreatic islets, MIN6 insulinoma cells and alpha-TC glucagonoma cells. All receptor mRNA levels were normalized to the level of GAPDH mRNA in the same tissue. *Black bars*, pancreatic islets; *hatched bars*, MIN6 cells; *double hatched bars*, alpha-TC cells.**

**Table 3 – GPR119 mRNA levels in various regions of the pancreas in humans.**

| Pancreatic region(s) | GPR119 mRNA level | n | P* |
|---|---|---|---|
| Head | 0.372±0.052 | 11 | - |
| Body | 0.294±0.069 | 6 | .388 |
| Tail | 0.262±0.079 | 2 | .367 |
| Body and tail | 0.286±0.053 | 8 | .264 |

GPR119 mRNA levels are expressed as means±SEM. Comparisons were made using unpaired two-tailed t tests.
* P values are vs the head.

between GPR119 mRNA expression and HbA1c levels and HOMA-IR values, which confirmed the absence of a significant correlation (Supplemental Table S1).

## 4. Discussion

Our findings demonstrate for the first time that *GPR119* is highly expressed in human pancreatic islets, where the level of *GPR119* expression is enriched more than 10-fold, as compared to adjacent areas of the pancreas in the same individuals. We also found that pancreatic levels of GPR119 mRNA are similar to those of GPR40 mRNA and are higher than those of GLP1R and SUR1 mRNA. Likewise, the level of GPR119 mRNA in isolated pancreatic islets is similar to that of GPR40 mRNA and higher than those of SUR1 and GLP1R mRNA [9,10]. This is noteworthy, as these receptors are reported to be abundantly expressed in human pancreatic islets.

We observed that substantial amounts of GPR119 mRNA are expressed in human insulinomas ($n=2$) and glucagonomas ($n=2$), and that the tumoral levels of the transcript are comparable to those in pancreatic islets. A similar pattern of GPR119 mRNA expression was also detected with mouse pancreatic islets, MIN6 insulinoma cells and alpha-TC glucagonoma cells. Thus GPR119 appears to be highly expressed in both beta and alpha cells in human and mouse pancreatic islets. Moreover, our observation that the expression levels of GPR119 and GPR40 mRNAs in human pancreatic islets are similar and are higher than that of SUR1 mRNA is noteworthy because SUR1 is reported to be abundantly expressed in both beta and alpha cells and is involved in the regulation of islet function, including insulin and glucagon secretion [38–40]. This strong expression suggests GPR119 may be involved in pancreatic islet function in humans. Consistent with that idea, pancreatic GPR119 mRNA levels correlated positively with two indices of beta cell function: the insulinogenic index and the HOMA-beta. Collectively, therefore, the present findings provide evidence for the possible involvement of GPR119 in islet function, perhaps affecting insulin secretion.

Using fresh tissue samples collected at surgery, we observed that, in humans, GPR119 mRNA is abundantly expressed in the small intestine, stomach and colon, but not in the esophagus. In rodents, GPR119 appears to be expressed in enteroendocrine cells, including L and K cells, and to be involved in the regulation of incretin and polypeptide YY secretion. In humans, enteroendocrine cells are distributed throughout the gastrointestinal tract, but not in the esophagus. Although details of GPR119 expression and its function in the human gastrointestinal tract will require further investigation, our findings are consistent with the idea that GPR119 is expressed in enteroendocrine cells and is involved in incretin and peptide YY secretion.

We detected no GPR119 mRNA in the human hypothalamus, brain or cerebrum, which is consistent with a recent report that GPR119 mRNA is not significantly expressed in the human brain or hypothalamus [19]. Although earlier reports using OEA (a putative GPR119 ligand) and a synthetic OEA analogue in rats suggest GPR119 may mediate signalling leading to reduced food intake and body weight, OEA appears

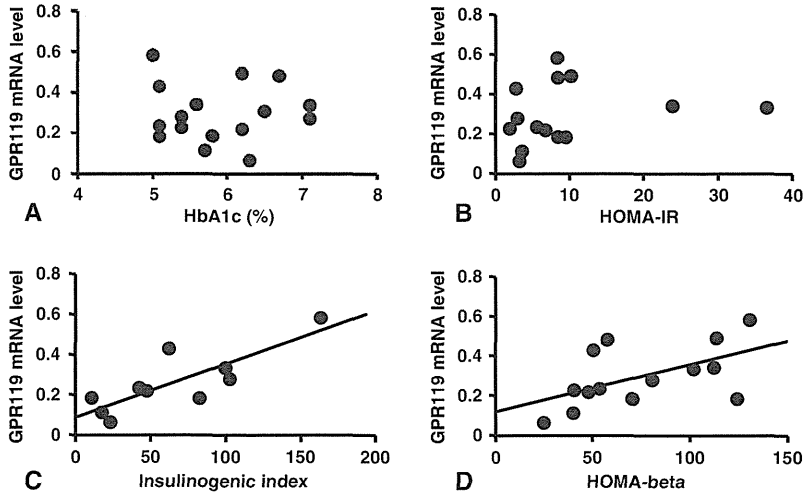


**Fig. 5 – Correlations between human pancreatic GPR119 mRNA levels and parameters of glucose metabolism, including HbA1c levels ($n=16$) (A), HOMA-IR values ($n=14$) (B), the insulinogenic index ($n=10$) (C) and HOMA-beta values ($n=14$) (D). All GPR119 mRNA levels were normalized to the level of GAPDH mRNA in the same tissue. Simple regression analysis was used to determine *P* and *r* values. The solid lines are regression lines.**

to act mainly in peripheral tissues, rather than in the central nervous system [41]. Our finding that GPR119 mRNA is highly expressed in the human stomach and duodenum is consistent with the notion that GPR119 is involved in regulating food intake in humans, as the bipolar vagal afferents involved in regulating feeding are known to project to the stomach and upper intestine [42,43].

In summary, the present study demonstrates that, in humans, GPR119 mRNA is abundantly expressed in healthy pancreatic islets and the human gastrointestinal tract, and in insulinomas and glucagonomas. The results provide evidence of an islet-gastrointestinal distribution of GPR119, its expression in pancreatic beta and alpha cells, and its possible involvement in islet function. They also provide the basis for a better understanding of the potential clinical importance of GPR119.

### 4.1. *Limitations of the present study*

Our study has several limitations that should be noted.

1. To our knowledge, no specific antibody against human GPR119 is available, so we were unable to assess expression of GPR119 protein.
2. The enrolled subjects were tumor-bearing patients, though the tumors were at an early stage or benign, and were resectable. Pancreatic biopsy is rarely performed because of the risk of pancreatitis, and is not justified in those without severe illness [44]. Therefore, we analyzed human pancreatic tissues collected during surgery. Because pancreatic tissue is very vulnerable to postmortem autolysis, specimens obtained at surgery offer substantial advantages for precise analysis of *GPR119* expression. Nonetheless, possible weight loss and the paracrine effects of pancreatic cancer cells on beta cells could have influenced the correlation study.
3. Patients enrolled in the present study were not severely diabetic (HbA1c was less than 7.2%), nor were they overweight or obese (BMIs were less than 25). Thus clarification of the pathophysiological role of GPR119 in human diabetes and obesity must await further investigation in patients with a wider range of glucose tolerances and BMIs.
4. Plasma glucagon levels were not determined in the preoperative evaluation, and were not included in the present study. Beta cell mass is known to be much greater than alpha cell mass in pancreatic islets, and correlations between GPR119 mRNA levels and indices for beta cell function seem plausible, but may underestimate the involvement of GPR119 in the glucagon secretion. Further studies will be necessary to clarify the role of GPR119 in glucagon secretion.

Supplementary materials related to this article can be found online at http://dx.doi.org/10.1016/j.metabol.2012.06.010.

## Author contributions

SO: data collection and analysis, data interpretation, manuscript writing. KH: data interpretation, manuscript writing. TT: data analysis, data interpretation, manuscript writing. JF, TK and KE: data interpretation, manuscript writing. YK, RD, KT, YS and SU: data collection, data interpretation. KN: data interpretation, manuscript writing.

## Funding

This work was supported in part by the Ministry of Education, Culture, Sports, Science and Technology of Japan; Ministry of Health, Labor and Welfare of Japan; Takeda Medical Research Foundation; Smoking Research Foundation; Suzuken Memorial Foundation; Japan Foundation of Applied Enzymology; Novo Nordisk Insulin Research award; and Lilly Education and Research Grant Office. We gratefully acknowledge cooperative research program FINDS with Shionogi & Co., Ltd.

## Acknowledgment

The authors acknowledge the technical assistance of Ms. A. Ryu of Kyoto University Graduate School of Medicine.

## Conflict of interest

The authors have no conflict of interest to declare.

## REFERENCES

[1] Stein DT, Stevenson BE, Chester MW, et al. The insulinotropic potency of fatty acids is influenced profoundly by their chain length and degree of saturation. J Clin Invest 1997;100:398–403.
[2] Lam TK, Pocai A, Gutierrez-Juarez R, et al. Hypothalamic sensing of circulating fatty acids is required for glucose homeostasis. Nat Med 2005;11:320–7.
[3] Fu J, Gaetani S, Oveisi F, et al. Oleylethanolamide regulates feeding and body weight through activation of the nuclear receptor PPAR-alpha. Nature 2003;425:90–3.
[4] Itoh Y, Kawamata Y, Harada M, et al. Free fatty acids regulate insulin secretion from pancreatic beta cells through GPR40. Nature 2003;422:173–6.
[5] Brown AJ, Goldsworthy SM, Barnes AA, et al. The orphan G protein-coupled receptors GPR41 and GPR43 are activated by propionate and other short chain carboxylic acids. J Biol Chem 2003;278:11312–9.
[6] Hirasawa A, Tsumaya K, Awaji T, et al. Free fatty acids regulate gut incretin glucagon-like peptide-1 secretion through GPR120. Nat Med 2005;11:90–4.
[7] Ahren B. Islet G protein-coupled receptors as potential targets for treatment of type 2 diabetes. Nat Rev Drug Discov 2009;8:369–85.
[8] Kebede MA, Alquier T, Latour MG, et al. Lipid receptors and islet function: therapeutic implications? Diabetes Obes Metab 2009;11(Suppl. 4):10–20.
[9] Tomita T, Masuzaki H, Iwakura H, et al. Expression of the gene for a membrane-bound fatty acid receptor in the pancreas and islet cell tumours in humans: evidence for GPR40 expression in pancreatic beta cells and implications for insulin secretion. Diabetologia 2006;49:962–8.